NASA CR-188335

Ball Aerospace Systems Group

Sc...
...7

FINAL STUDY REPORT
DRL 8

DEBRIS COLLISION WARNING SENSOR
PHASE B-3 STUDY

CONTRACT NAS9-18346
MODIFICATIONS 10, 11 and 12

(NASA-CR-188335) DEBRIS COLLISION WARNING SENSOR, PHASE B-3 STUDY (Diskette Supplement) Final Study Report (Ball Aerospace Systems Div.) 69 p

N95-70263

Unclas

Z9/19 0027701

PREPARED FOR
NASA LYNDON B. JOHNSON SPACE CENTER
HOUSTON, TEXAS

PREPARED BY
BALL ELECTRO-OPTICS/CRYOGENICS DIVISION
PO BOX 1062
BOULDER, CO 80303

DECEMBER, 1992

Electro-Optics/Cryogenics Division
P.O. Box 1062, Boulder, Colorado 80306-1062 (303) 939-4000 TWX: 910-940-3241 Telex: 45-605 FAX: (303) 442-4812

FINAL STUDY REPORT
DRL 8

DEBRIS COLLISION WARNING SENSOR
PHASE B-3 STUDY

CONTRACT NAS9-18346
MODIFICATIONS 10, 11 and 12

PREPARED FOR
NASA LYNDON B. JOHNSON SPACE CENTER
HOUSTON, TEXAS

PREPARED BY
BALL ELECTRO-OPTICS/CRYOGENICS DIVISION
PO BOX 1062
BOULDER, CO 80303

DECEMBER, 1992

FOREWORD

Ball Electro-Optics/Cryogenics Division (BECD) is pleased to submit this final report of the Phase B-3 concept study of the Debris Collision Warning Sensor (DCWS) for the NASA Lyndon B. Johnson Space Center.

Our report is submitted in one document:

* **DCWS Phase B-3 Study Final Report**

EXECUTIVE SUMMARY

The DCWS Phase B study has been divided into three segments, arbitrarily defined as:

* Phase B
* Phase B-2
* Phase B-3

PHASE B

The DCWS Phase B study results provided an instrument concept consistent with the Johnson Space Center (JSC) Request for Proposal (RFP) 9-BE3-02-9-47P, dated November 7,1989, and subsequent revisions developed during the course of the study.

In accordance with the original contract and Modifications 1 through 5, BECD identified and defined a means of meeting the complete program science requirements, including cold particle detection in a significantly smaller, 60cm, optical system than anticipated in the Phase A Study, which required a 160cm telescope. The Phase B study effort was reported in DRL 8 Final Report, "Debris Collision Warning Sensor Phase B Instrument Concept Report", dated April 1991.

PHASE B-2

Contract modifications 6 through 11 directed a study of experiment cost reduction options including:

* Examination of experiment and performance requirements as cost drivers.
* Identify cost reduction options for potential impacts on science objectives, instrument and/or operational capabilities.
* Examine other than STS experiment flight options, such as a free-flyer or Space Station Freedom (SSF) attached payload.
* Generate a summary report and phase C/D estimates for the recommended approach(s).

A summary of the B-2 study results are:

Analysis of the white light and infrared channels show that allowing an increase in observation time, up to the 50 to 100 hour range, and the elimination of in-plane, depressed angle and USSSPACECOM observations will allow significant reduction of instrument size. Smaller instrument apertures allow the use of refractive, rather than reflective optics and the separation of the infrared and white light bands into separate telescopes. The baseline system resulting from the analysis uses a 15cm aperture for the white light band and a 20cm aperture for the combined infrared bands. These changes, in turn, reduce the cryogenic cooling requirements and result in the simplification and size reduction of the cryogenics subsystem. The modifications to the experiment observing requirements have provided an opportunity to reduce the basic DCWS instrument size, cost and increase it's adaptability to alternate flight platform interface and operational requirements.

In addition to reducing the aperture diameters, the telescope and light shade lengths were shortened sufficiently to reduce the overall instrument length, including the cryogen tank, to about 3.5m. This reduction in length made it feasible to mount the instrument on a Explorer class free flyer or to be mounted transversely in the STS orbiter bay. The transverse bay mounting allows the use of a TAPS payload pointing system, rather than the more expensive IPS, and reduces the bay length and cost, required for launch of the instrument system. The TAPS does not provide three axis pointing, as does the IPS, but there is sufficient space in the TAPS to include a roll ring with the instrument.

In summary, extending the allowable observation hours and eliminating some observing modes allowed the DCWS instrument system size to be reduced sufficiently to fit the physical limits of an Explorer class free flyer or a TAPS pointing system on the STS. The size reduction was not a major constraint for use on SSF but it did reduce the costs and logistics problems inherent in the launch of the instrument and the integration of the instrument to the station.

The "Debris Collision Warning Sensor Phase B-2 Final Report" was submitted in December 1991.

PHASE B-3

Contract modification 12, dated June 7,1991, directed a continuation of DCWS Phase B concept definition allowing potential additional cost reductions including:

* Definition of a Technology Demonstration Systems Concept.
* Evaluation of Standard Parts and "Off-The-Shelf" NASA and DOD instrument systems for application to the DCWS science requirements.

Contract funding limitations restricted the Phase B-3 effort to a cursory evaluation of two DOD instrument systems, CIRRIS-1 and FIRSSE. The results of that evaluation was reported as DRL 2, "DCWS Interim Report on Existing Telescopes and Systems for Accomplishment of the DCWS Mission" on November 16, 1992. That effort exhausted the available contract funds, and in accordance with technical direction the Phase B-3 Final Report is comprised of:

* The Executive Summary;

* The DCWS Interim Report on Existing Telescopes and Systems for Accomplishment of the DCWS Mission;

* The Model of the DCWS system developed during Phases B and B-2, on the enclosed disc, consisting of:

  - DCWSVM1.WQ1, Visible sensor model in Quattro Pro format as described in System Engineering Report (SER) DCWS -91.001.PS, dated January 10, 1991 (Appendix A). This model assumes a 57 degree, 500 km orbit in 1995.

  - DCWSVM2.WQ1, the same model as DCWSVM1, except for a 28 degree, 420km orbit in 1997.

  - IRSCALE1.WQ1, Infrared sensor scaling model in Quattro Pro format, used in conjunction with Ball proprietary program IRSENSOR to predict performance of the infrared DCWS sensor. This model is described in SER DCWS-91003.PS, dated February 20 1991 (Appendix B). This model assumes a 57 degree, 500km orbit in 1997.

  - IRSCALE2.WQ1, The same model as IRSCALE2, except for 28 degree,420km orbit in 1997.

  - DEBRISA.MCD, a Mathcad Ver.3.1 model showing how weighted averages of debris models used in DCWSVM1.WQ1 and IRSCALE1.WQ1 were calculated.

  - DEBRISB.MCD, a Mathcad Ver.3.1 model showing how weighted averages of debris models used in DCWSVM2.WQ1 and IRSCALE2.WQ1 were calculated.

  - DEBRIS1.MCD, a Mathcad Ver.3.1 model showing how the range correction factor (to account for altitude vs. range effect) used in DCWSVM1.WQ1 and IRSCALE1.WQ1 were calculated.

  - DEBRIS2.MCD, a Mathcad Ver.3.1 model showing how the range correction factor (to account for altitude vs. range effect) used in DCWSVM2.WQ1 and IRSCALE2.WQ1 were calculated.

DCWS Interim Report

on

Existing Telescopes and Systems for Accomplishing the DCWS Mission

November 13, 1992

Prepared for

NASA Lyndon B. Johnson Space Center
Houston, Texas 77058

Prepared by

Paul W. Scott and Becky A. Benedict
Ball Electro-Optics and Cryogenics Division
P.O. Box 1062
Boulder, Colorado 80306

Under NASA Contract Number NAS9-18346
Contract Amendment Number 12

Introduction and Summary

The result of the extended Phase B Study for the Debris Collision Warning Sensor (DCWS) program was recommendation for a visible telescope with a 15 cm aperture, and a two focal plane, two band (6 - 9 microns MWIR, and 9 - 12 microns LWIR) infrared telescope with a 20 cm aperture. The infrared telescope is proposed to be cooled using ScHe stored in an on-gimbal tank of a modified Power Reactant Storage Assembly (PRSA) design. This was proposed to replace the baseline 60 cm common telescope configuration with off-gimbal ScN_2 telescope cooling and on-gimbal ScHe focal plane cooling.

In the ongoing efforts to accomplish the DCWS mission at a reduced cost, Ball Electro-optics and Cryogenics Division (BECD) has explored several possiblities for the use of existing instruments for the infrared portion of the DCWS mission. Part of the original statement of work for this contract modification was to explore the Cryogenic InfraRed Radiance Instrumentation for Shuttle (CIRRIS)-1A instrument as an alternative. Initial investigation into this option revealed that major modifications to the instrument, including replacement of the focal plane with an entirely different type of focal plane, would be required to make the instrument meet our functional requirements, and even then it would have insufficient aperture and field of view to complete the mission in a reasonable number of hours. However, two other instruments, Survey Probe Infrared Celestial Experiment (SPICE) and Far InfraRed Sky Survey Experiment (FIRSSE), were found to exist at the Air Force Geophysics Laboratory (AFGL), now a part of the Air Force Phillips Laboratory. They are not currently being used and have more potential for the DCWS application. The most information was available about FIRSSE, for which Ball built the dewar and cold baffle system and integrated it with the telescope. Of the information we do have on SPICE, it appears that it does not have sufficient spatial resolution for the DCWS application, partly due to excessive central obscuration, and there is an open question about mirror stability at cold temperatures.

We therefore concentrated most of our effort during the last part of the study on the FIRSSE instrument. The conclusion reached is that the FIRSSE optics have appropriate parameters for doing the DCWS mission, but the focal plane would have to be replaced, a cryogenic study is required to arrive at the best solution to cooling the telescope for a Shuttle mission, and interfaces would have to be designed to mount the instrument in an appropriate gimbal, presumably the TAPS. These general conclusions apply also to SPICE. The existing FIRSSE dewar alone is clearly inadequate due to limited hold time and limited on-orbit mission life. Using the FIRSSE system allows DCWS to use an existing optical subsystem, but the money and time saved by doing so may or may not be equal to the extra effort required to adapt the rest of the system to those optics. The existing optics are not now qualified for a Shuttle application, and so that cost, schedule, and risk would also have to be considered. The fact that the FIRSSE optics must run colder, and do not have a warm baffle/cold baffle configuration may require more cryogen storage and may aggravate the contamination problems.

Optical Design Parameters - DCWS Phase B2 vs. CIRRIS-1A vs. FIRSSE

Table I shows a comparison of the basic optical design parameters for the DCWS Phase B2, the CIRRIS-1A, and the FIRSSE instruments. Clearly, the CIRRIS-1A instrument is inferior to the other two in terms of both field of view and collecting aperture, which are directly related to performance, although the advantage of CIRRIS-1A is that it is already Shuttle-qualified, at least in its current configuration, and is interfaced to a Shuttle pointing system. Another disadvantage of CIRRIS-1A is that it is currently planned for upgrade and use, and is not as available for a total reconfiguration.

Table I. First order optical parameters of the DCWS Phase B-2, CIRRIS-1A, and FIRSSE systems. The FIRSSE system is assumed to use the same focal plane as the DCWS Phase B-2 system.

Parameter	DCWS Phase B2 Value	CIRRIS-1A Value	FIRSSE Value With DCWS FPA
Focal length (cm)	25.42	61	86.41
Field of View (deg)	4.33 x 2.17	1.26 x 0.17 (disc. detectors)	1.273 x 0.636
IFOV (microradians)	295	500	86.8
Clear aperture (cm)	20	7.65 , D-shaped (equivalent)	36
Focal Ratio	1.27	Non-symmetrical	2.4
Obscuration Ratio	0	0 (equivalent)	0.48
Focal Plane Configuration (single FPA)	Two 128 x 128 arrays with 75 micron pixels	5 discrete detectors (various sizes)	Two 128 x 128 arrays with 75 micron pixels

Performance modeling - DCWS Phase B2 vs. FIRSSE

Performance models similar to those carried out on the DCWS Phase B2 program were exercised with respect to the FIRSSE system, and updated for the DCWS Phase B2 system. Each system was analyzed the number of hours required to meet the DCWS requirements of detecting, with a single-pixel SNR of 1 and an event SNR of 10, at least 100 ideal 300 K particles between 1mm and 1cm, at least 500 particles between 1 cm and 3 cm, and 200 particles between 3 cm and 10 cm. The FIRSSE model was done assuming 20 K optics with a 10 K focal plane. The original FIRSSE ran at lower temperatures for both optics and focal plane, but the 20 K optics contribute no noise to the focal plane, and a temperature of around 10 K is required to operate the DCWS focal plane, which was assumed to be used in both instruments. The only differences between the focal planes for the two instruments are that, since the FIRSSE instrument is much colder, a broader set of wavelength bands was selected going out to 16 microns and since the FOV of the FIRSSE instrument is smaller, a shorter integration time was chosen (6.5 msec, vs. 20 msec for DCWS) . Even longer wavelengths are possible. Performance of the FIRSSE instrument with the same wavelength bands as DCWS was inferior to DCWS, due to the narrower field of view, but superior performance can be achieved by taking advantage of the colder temperature to extend the bands. The DCWS system was designed to operate at around 75 K. However, thermal calculations made at the end of the Phase B2 study, after eliminating two arrays from the focal plane, indicated that the instrument may run closer to 55 - 60 K.

We therefore compare here three cases: FIRSSE at 20 K with wavebands of 6 - 11 and 11 - 16 microns, DCWS at 75 K with wavebands of 6 - 9 microns and 9 - 12 microns, and DCWS at 55/60 K with wavebands of 6 - 9 microns and 9 - 12 microns. At 55/60 K, the DCWS system could be improved further by increasing the wavelength bands, if required, but optical design changes would be required. Details of the models used are included in Appendix A, and the results are given in Tables II and III. The significant result is that the FIRSSE instrument can exceed the DCWS requirements, particularly for colder particles, if it can be cooled to a significantly lower temperature than that assumed for DCWS. A complete analysis of the required temperature for the FIRSSE instrument has not been completed at this time. One of the key issues to be addressed in the substitution of the FIRSSE instrument for the DCWS Phase B2 design is whether there is a feasible and cost-effective means to cool the FIRSSE instrument over the required mission life.

Table II. Predicted observation time required to observe the DCWS required warm (300 K) particle counts.

	500 km, 57 Deg Orbit 1995		420 km, 28.5 Deg Orbit 1997	
	MWIR	LWIR	MWIR	LWIR
FIRSSE at 20 K	40	38	53	50
DCWS at 75 K	40	55	55	76
DCWS at 55/60 K	39	13	54	19

Table III. Predicted cold (240 K) particle counts corresponding to the hours listed in Table II.

	Particle Size	500 km, 57 Deg Orbit 1995		420 km, 28.5 Deg Orbit 1997	
		MWIR	LWIR	MWIR	LWIR
FIRSSE at 20 K	1-10 mm	5	16	5	15
	10-30 mm	46	106	43	102
	30-100 mm	604	1029	621	1177
DCWS at 75 K	1-10 mm	2	6	2	6
	10-30 mm	29	67	29	67
	30-100 mm	514	1046	568	1183
DCWS at 55/60 K	1-10 mm	2	8	2	9
	10-30 mm	29	61	28	67
	30-100 mm	510	652	568	845

Cryogenic Issues for FIRSSE

It was not possible in the time available to perform enough analysis to confirm any one concept for cooling the FIRSSE instruments. However, we have held discussions with Becky Benedict, the cryogenic engineer for DCWS, and Jim Lester, the primary developer of the FIRSSE dewar and cold baffle, and arrived at a number of candidate concepts, some of which make use of the existing FIRSSE dewar, augmented by additional hardware. A cutaway view of the FIRSSE system is shown in figure 1, with added callouts to show the cryogenic system features. A summary of the cryogenic system design features is included in Appendix B. The existing dewar was designed for a very short hold time and life, since it was launched on a sounding rocket, and a large amount of superfluid helium would be required to replenish the existing system for a longer time. In addition, the required focal plane for DCWS will consume much more power than the original FIRSSE focal plane. Each alternative approach involves some level of risk, such as on-orbit fluid transfer. The FIRSSE telescope was built first by Perkin-Elmer and retrofitted by Ball with its cryogenic system, producing a modular system, so an entirely new cryogenic system could be devised for the existing telescope and the new focal plane.

The basic cryogenic options are listed in Table IV, along with advantages, disadvantages, and risks associated with each. The first option, to use FIRSSE in its design configuration, is not really an option, since it will not work, due to insufficient hold time and insufficient experiment time. The second option makes use of the Spacelab Superfluid Helium Experiment Dewar (SSHED), a 110-liter SfHe experiment dewar that flew on Spacelab, and is therefore Shuttle-qualified. The SSHED dewar is currently at JPL, being used for the Lambda-Point Shuttle mission. This option requires on-orbit SfHe transfer from SSHED to the FIRSSE dewar, which is well understood by Ball, but the technology has not been demonstrated in space. It would require modification of FIRSSE for baffle and plumbing interfaces. Another option is to use one or two PRSA Hydrogen tanks filled with ScHe on the new Extended Duration Orbiter (EDO) pallet. This requires modifying the FIRSSE plumbing, a new PRSA interface, new plumbing between PRSA and FIRSSE interfaces, and modifying FIRSSE to have a He vapor cooled upper baffle. How much re-qualification would be required and the mission impact of pre-empting EDO dewars would be a major issue. The fourth option would be to use the FIRSSE dewar with SfHe and cool the upper baffle with N_2 vapor. SSHED would be used in this case for the SfHe, with on-orbit transfer to FIRSSE, and a Space Station Fluid Tank Set (FTS) dewar or another SSHED dewar could be used to store the N_2 as ScN_2.

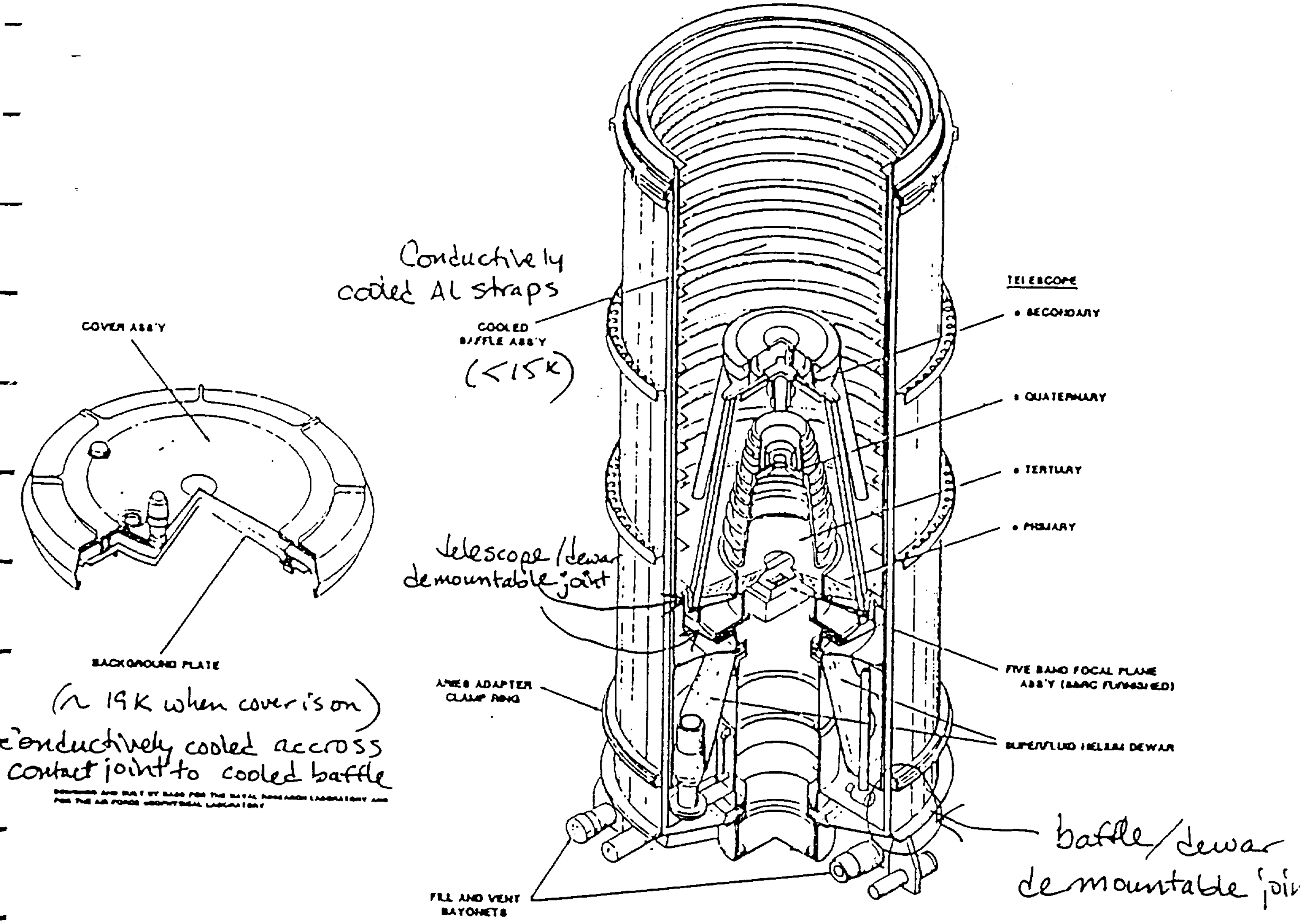

Figure 1. FIRSSE Cryogenic System

Table IV. Tradeoff options for a cryogenic system to support the FIRSSE Telescope for a DCWS mission on the Space Shuttle.

Option	Advantages	Disadvantages	Risk
1) FIRSSE - Use FIRSSE as is with SfHe	- Adequate telescope performance for DCWS - Designed for SfHe, a good coolant - Hardware is flight quality and still exists - Partial cooldown prior to launch - Hardware is modular and can be refurbished	- Needs qualification for Shuttle; is flight hardware for rocket-borne launch - Only 100 min max hold time (vent closed) from last vacuum service to open vent to space after launch. - Only holds 17 liters SfHe when full, need >100 liters, provides only 10 hrs. observation time - Upper baffle runs cooler than required, wasting SfHe - Requires on-orbit cooldown	Will not work
2) FIRSSE & SSHED - Use FIRSSE dewar with SfHe - Modify with upper baffle He VCS - Modify FIRSSE plumbing - Use existing SSHED - Do on-orbit SfHe transfer from SSHED to FIRSSE	- Uses 2 existing systems, 1 is Shuttle qualified - May be low-cost - On-orbit transfer is believed to be easy - Partial cooldown prior to launch	- Requires qualification of FIRSSE for Shuttle - Requires mod of FIRSSE for baffle and plumbing interface - On-orbit transfer never done before	Med
3) FIRSSE & EDO - Use FIRSSE with ScHe - Use 1 or 2 H_2 PRSA tanks on EDO pallet, but fill with ScHe - Modify FIRSSE plumbing - New PRSA interface - New plumbing from FIRSSE to PRSA interface - Modify FIRSSE with He vapor-cooled upper baffle - Transfer ScHe from PRSA dewars to FIRSSE passively	- Uses 2 existing dewars, one qualified - Partial cooldown prior to launch	- Moderate to high cost - Need stress analysis to prove qualification of He instead of H_2 for PRSA (weight, vib) - Need to assess impact of using existing EDO Shuttle hardware other than intended	High

Option	Advantages	Disadvantages	Risk
4) FIRSSE & 2 SSHED - Use FIRSSE with SfHe and use N_2 vapor for baffle cooling - Modify FIRSSE plumbing and upper baffle - Use existing SSHED - Do on-orbit SfHe transfer from SSHED to FIRSSE - Build new SSHED using existing design but use with N_2 vapor for baffle cooling	- Uses 2 existing dewars, one qualified - ScN_2 provides additional coolant to He vapor in option 2 - Moderate cost - Partial cooldown prior to launch	- 3 dewars, more weight than option 2 - Need to build another SSHED, same design - Need to qualify new SSHED for ScN_2 - Small gas line for N_2 vapor across gimbal - Pressure drop and parasitic heat load in plumbing across gimbal	Med
5) FIRSSE, SSHED & FTS - Use FIRSSE with SfHe and N_2 vapor for baffles - Modify FIRSSE plumbing and upper baffle - Use existing SSHED - Do on-orbit SfHe transfer from SSHED to FIRSSE - Use existing FTS ScN_2 dewar with N_2 vapor for baffle cooling	-Uses 3 existing dewars, 1 qualified, 1 in '93 qualification for Space Station - Uses all dewars as designed - Low cost - Partial cooldown prior to launch	- 3 dewars, more weight than option 2 - Small gas line for N_2 vapor across gimbal	High
6) SSHED & He JT - Use SSHED with S-Ne - Use He in high pressure gas bottle for FPA cooling and vapor for cooling telescope/baffles - May use gas Ne for baffle cooling	- Existing qualified dewar - Low cost JT cryo system	- Need to analyze SSHED cryo system with S-Ne - Need stress analysis to prove qualification of SSHED with S-Ne (weight, vib) - Small gas line for He (and maybe Ne) across gimbal - On-orbit cooldown	Low

Option	Advantages	Disadvantages	Risk
7) Custom & SSHED - Use custom dewar with ScHe - Use existing SSHED - Do on-orbit SfHe transfer from SSHED to custom dewar	-Uses 2 dewars - Reduces weight - Uses all dewars as designed - Does not require mods to existing hardware or shuttle PRSA system - No lines across gimbal during operation - Moderate cost - Partial cooldown prior to launch - Less weight on-gimbal than option 8	-Specialized build & qualification of dewar/telescope - Does not use as much existing hardware	Low
8) Custom - Use custom dewar with ScHe	- Uses 1 dewar - Minimizes total weight over option 7 - Does not require mods to existing hardware or shuttle PRSA system - No lines across gimbal during operation - No on-orbit SfHe transfer - Complete cooldown prior to launch - Long hold time prior to launch	- Moderate to high cost - Specialized build & qualification of dewar/telescope - Does not use existing hardware - More weight on-gimbal	Lowest

The remaining options would make use only of the FIRSSE telescope and structure, with no use made of the FIRSSE dewar or baffle. They also could be accomplished with another telescope. The first of these would use solid neon in a SSHED in conjunction with a high pressure gas bottle of He to cool the FPA and then provide vapor cooling for the telescope and baffles. Neon gas could also be used to cool the baffles. No new dewar would have to be qualified for this approach. However, the existing SSHED design would have to be analyzed for substitution of S-Ne for SfHe. Option 6 could also look at the use of the Ball S-Ar dewar (flown on the Shuttle Broad Band X-Ray Telescope experiment), substituting Ne for Ar. The other two options would involve custom dewar designs. They would be lower risk options, but with higher cost.

If the FIRSSE concept is pursued for DCWS, there are several other existing SfHe dewars that warrant further study as FIRSSE resupply dewars. NASA's SfHe On-Orbit Transfer (SHOOT) will demonstrate SfHe transfer in space and is scheduled for a Shuttle launch mid-1993.

SHOOT is being developed by M. DiPirro and S. Castles (NASA/Goddard) and its SfHe dewars may be good candidates for DCWS. IR telescope (IRT) is a NASA/Marshall Shuttle-based He cooled telescope built/launched in the mid '80s. We need to gather more information on that experiment, but we currently understand that two dewars existed and that SfHe was stored and then used for gas cooling of the telescope system. Apparently Eugene Urban (Marshall) and Frank Low (U. of Arizona) helped develop the IRT.

Balll has extensive in-house experience with SfHe modeling, analysis, fluid transfer in our labs, and we successfully developed the dewar for SSHED. Ball SfHe usage and cryogenic system development continues with studies on fluid transfer in space and development efforts for SfHe dewars for other space applications (such as the X-ray Spectrometer (XRS) dewar for AXAF, Superfluid Helium Tanker (SHFT), SPIRIT III (SDIO experiment), Astromag, COLD-SAT, and SIRTF studies). In space applications, SfHe can be transferred between tanks passively by using a thermomechanical pump (no moving parts). SfHe has been transferred in labs since the 1930's and here at Ball in small and large scale (80 liters). This experience leads us to believe that SfHe transfer is a manageable technology for space applications and it is less complicated and costly than resupply of other cryogenic fluids in other phases (i.e., supercritical or liquid).

In summary from the cryogenic system perspective, the FIRSSE system alone (option 1) will not work for DCWS. The use of FIRSSE and SSHED hardware (option 2) with on-orbit transfer/resupply of SfHe is perhaps the best low cost approach and only assumes moderate risk. Of the concepts studied, the custom integral dewar/telescope design (option 8) appears to be the lowest risk approach but is as the moderate to high cost level. These cryogenic trades are preliminary and more refined analysis and full cost trades are needed to make more accurate and quantitative judgements.

Pointing Issues

There are several obvious conclusions that can be drawn regarding pointing implications of the alternate instrument options. First, as opposed to the DCWS designs and the CIRRIS-1A instrument, the FIRSSE or SPICE designs would have to include interfacing to a Space Shuttle gimbal. Presumably either could be retrofitted to the TAPS gimbal, but no real investigation of this potential has been undertaken. Second, the narrower field of view and IFOV for the FIRSSE design will produce a proportionally tighter pointing control requirement on the system. We do not believe this is a critical issue.

Summary

It should be noted that all of the cryogenic options presented imply a certain amount of additional risk over the DCWS Phase B2 design, and none have been analyzed so far to show feasibility. In all cases there is a risk that the FIRSSE system will not be qualifiable for the Shuttle environment. In addition, each option requires either modification to the FIRSSE hardware, modifications to existing hardware which may affect its qualification status, or major new hardware. BECD cannot recommend dropping the current design in favor of any of these options at this point without significant further investigation, including analysis as well as design and cost tradeoffs. Since the acceptability of the FIRSSE telescope configuration relies on a lower temperature and the existing cryogenic system is inadequate, the tradeoff is essentially in the area of cryogenics and the potential for cost savings. It is not clear at this point whether or not there is a feasible cryogenic system for the FIRSSE telescope that will save money or even be as cost effective as the Phase B2 design.

Potentially, under the best of conditions, schedule could be saved by using an existing set of optics. However, there is a high degree of uncertainty as to the actual schedule savings due to the uncertainty regarding the cryogenic retrofit approach, the schedule required in order to confirm the viability of a cryogenic approach, and the extent to which the telescope hardware build is on the program critical path. Therefore, we would not see schedule savings as a driving reason to select a pre-existing telescope at this time. However, if the cryogenic issues were resolved before the program starts, a true schedule savings may be revealed.

Appendix A.

IRSENSOR Models

IRSENSOR VERSION 2.1 04/30/91

CURRENT DATE: 09/22/92
CURRENT TIME: 09:57

DCWS 6-9 microns, 60/55 K, 20 msec frame time, .01 unshielded structure

INPUT DATA

SENSOR DATA:	
SENSOR TYPE (Stare:LinearScan:CircularScan)	S
STARE TIME AVAILABLE	2.000E-02 sec
FIELD OF VIEW - AZIMUTH	4.326 degrees
FIELD OF VIEW - ELEVATION	4.326 degrees
IFOV - AZIMUTH	2.950E-04 radians
IFOV - ELEVATION	2.950E-04 radians
RANGE TO TARGET	100.0 km
RADIOMETRIC DATA:	
BACKGROUND TYPE (Inband : Spectral : Greybody)	S
BACKGROUND SPECTRAL RADIANCE	5.100E-11 W/cm2.sr.u
TARGET TYPE (Point : Xtended : Star)	P
TARGET TEMPERATURE	300.0 K
TARGET AREA-EMISSIVITY PRODUCT	7.070E-01 cm2
FOREGROUND TYPE (Inband : Spectral)	I
FOREGROUND INBAND RADIANCE	0.000E+00 W/cm2.sr
FOREGROUND TRANSMISSION	1.000
WARM OPTICS TRANSMISSION	0.729
WARM OPTICS EMISSIVITY	0.271
WARM OPTICS TEMPERATURE	60 K
COLD OPTICS SPECTRAL TYPE (Wide : Narrow)	W
COLD OPTICS CUT-ON WAVELENGTH	6.000 um
COLD OPTICS CUT-OFF WAVELENGTH	12.000 um
COLD OPTICS TRANSMISSION	0.857
COLD OPTICS EMISSIVITY	0.143
COLD OPTICS TEMPERATURE	55 K
UNSHIELDED STRUCTURE TEMPERATURE	60 K
UNSHIELDED STRUCTURE EMISSIVITY	1.000
UNSHIELDED SOLID ANGLE at DETECTOR	0.010 sr
CENTRAL OBSCURATION TEMPERATURE	55 K
CENTRAL OBSCURATION EMISSIVITY	1.000
COLD FILTER SPECTRAL TYPE (Wide : Narrow)	W
COLD FILTER CUT-ON WAVELENGTH	6.000 um
COLD FILTER CUT-OFF WAVELENGTH	9.000 um
COLD FILTER TRANSMISSION	0.910
COLD FILTER EMISSIVITY	0.050
COLD FILTER TEMPERATURE	20 K
OPTICS DATA:	
COLLECTING OPTICS DIAMETER	20.0 cm
LINEAR OBSCURATION RATIO	0.000
POINT SOURCE COLLECTION EFFICIENCY (ref diff limit	1.000

DCWS 6-9 microns, 60/55 K, 20 msec frame time, .01 unshielded structure

INPUT DATA CONTINUED:

DETECTOR DATA:

DETECTOR MATERIAL (INSB, HGCDTE, SILICON)	Si:A
DETECTOR SIZE - AZIMUTH	75 um
DETECTOR SIZE - ELEVATION	75 um
DETECTOR THICKNESS	20 um
DETECTOR ACTIVE AREA RATIO (fill factor)	1.000
DETECTOR TEMPERATURE	10.0 K
DETECTOR CUTOFF WAVELENGTH	27.0 um
DETECTOR QUANTUM EFFICIENCY (default=TABLE)	0.5500
DETECTOR 1/f NOISE BREAK FREQ	0.000E+00 Hz
DETECTOR MODE (PV, PC, XX)(Default=PV)	PV
DETECTOR RoA PRODUCT (default=CALCULATED)	2.000E+06 Ohms.cm2
DETECTOR CAPACITANCE (default=TABLE)	5.0 pF
DETECTOR DARK CURRENT	0.000E+00 Amp

CHARGE INTEGRATING PREAMP INPUT DATA:

DETECTOR FULL WELL CAPACITY	1.000E+06 e-/pixel
ARRAY READ-OUT NOISE	50 e- rms

IRSENSOR VERSION 2.1 04/30/91

CURRENT DATE: 09/22/92
CURRENT TIME: 09:53

DCWS 9-12 microns, 60/55 K, 20 msec frame time, .01 unshielded structur

INPUT DATA

SENSOR DATA:	
SENSOR TYPE (Stare:LinearScan:CircularScan)	S
STARE TIME AVAILABLE	2.000E-02 sec
FIELD OF VIEW - AZIMUTH	4.326 degrees
FIELD OF VIEW - ELEVATION	4.326 degrees
IFOV - AZIMUTH	2.950E-04 radians
IFOV - ELEVATION	2.950E-04 radians
RANGE TO TARGET	100.0 km
RADIOMETRIC DATA:	
BACKGROUND TYPE (Inband : Spectral : Greybody)	S
BACKGROUND SPECTRAL RADIANCE	9.900E-11 W/cm2.sr.u
TARGET TYPE (Point : Xtended : Star)	P
TARGET TEMPERATURE	300.0 K
TARGET AREA-EMISSIVITY PRODUCT	7.070E-01 cm2
FOREGROUND TYPE (Inband : Spectral)	I
FOREGROUND INBAND RADIANCE	0.000E+00 W/cm2.sr
FOREGROUND TRANSMISSION	1.000
WARM OPTICS TRANSMISSION	0.729
WARM OPTICS EMISSIVITY	0.271
WARM OPTICS TEMPERATURE	60 K
COLD OPTICS SPECTRAL TYPE (Wide : Narrow)	W
COLD OPTICS CUT-ON WAVELENGTH	6.000 um
COLD OPTICS CUT-OFF WAVELENGTH	12.000 um
COLD OPTICS TRANSMISSION	0.857
COLD OPTICS EMISSIVITY	0.143
COLD OPTICS TEMPERATURE	55 K
UNSHIELDED STRUCTURE TEMPERATURE	60 K
UNSHIELDED STRUCTURE EMISSIVITY	1.000
UNSHIELDED SOLID ANGLE at DETECTOR	0.010 sr
CENTRAL OBSCURATION TEMPERATURE	55 K
CENTRAL OBSCURATION EMISSIVITY	1.000
COLD FILTER SPECTRAL TYPE (Wide : Narrow)	W
COLD FILTER CUT-ON WAVELENGTH	9.000 um
COLD FILTER CUT-OFF WAVELENGTH	12.000 um
COLD FILTER TRANSMISSION	0.910
COLD FILTER EMISSIVITY	0.050
COLD FILTER TEMPERATURE	20 K
OPTICS DATA:	
COLLECTING OPTICS DIAMETER	20.0 cm
LINEAR OBSCURATION RATIO	0.000
POINT SOURCE COLLECTION EFFICIENCY (ref diff limit	1.000

DCWS 9-12 microns, 60/55 K, 20 msec frame time, .01 unshielded structure

INPUT DATA CONTINUED:

DETECTOR DATA:

DETECTOR MATERIAL (INSB, HGCDTE, SILICON)	Si:A	
DETECTOR SIZE - AZIMUTH	75	um
DETECTOR SIZE - ELEVATION	75	um
DETECTOR THICKNESS	20	um
DETECTOR ACTIVE AREA RATIO (fill factor)	1.000	
DETECTOR TEMPERATURE	10.0	K
DETECTOR CUTOFF WAVELENGTH	27.0	um
DETECTOR QUANTUM EFFICIENCY (default=TABLE)	0.6500	
DETECTOR 1/f NOISE BREAK FREQ	0.000E+00	Hz
DETECTOR MODE (PV, PC, XX)(Default=PV)	PV	
DETECTOR RoA PRODUCT (default=CALCULATED)	2.000E+06	Ohms.cm2
DETECTOR CAPACITANCE (default=TABLE)	5.0	pF
DETECTOR DARK CURRENT	0.000E+00	Amp

CHARGE INTEGRATING PREAMP INPUT DATA:

DETECTOR FULL WELL CAPACITY	1.000E+06	e-/pixel
ARRAY READ-OUT NOISE	50	e- rms

IRSENSOR VERSION 2.1   04/30/91

CURRENT DATE: 10/08/92
CURRENT TIME: 10:43

DCWS 6-9 microns, 75 K, 20 msec frame time, .01 unshielded structure

INPUT DATA

SENSOR DATA:

SENSOR TYPE (Stare:LinearScan:CircularScan)	S
STARE TIME AVAILABLE	2.000E-02 sec
FIELD OF VIEW - AZIMUTH	4.326 degrees
FIELD OF VIEW - ELEVATION	4.326 degrees
IFOV - AZIMUTH	2.950E-04 radians
IFOV - ELEVATION	2.950E-04 radians
RANGE TO TARGET	100.0 km

RADIOMETRIC DATA:

BACKGROUND TYPE (Inband : Spectral : Greybody)	S
BACKGROUND SPECTRAL RADIANCE	5.100E-11 W/cm2.sr.u
TARGET TYPE (Point : Xtended : Star)	P
TARGET TEMPERATURE	300.0 K
TARGET AREA-EMISSIVITY PRODUCT	7.070E-01 cm2
FOREGROUND TYPE (Inband : Spectral)	I
FOREGROUND INBAND RADIANCE	0.000E+00 W/cm2.sr
FOREGROUND TRANSMISSION	1.000
WARM OPTICS TRANSMISSION	0.729
WARM OPTICS EMISSIVITY	0.271
WARM OPTICS TEMPERATURE	75 K
COLD OPTICS SPECTRAL TYPE (Wide : Narrow)	W
COLD OPTICS CUT-ON WAVELENGTH	6.000 um
COLD OPTICS CUT-OFF WAVELENGTH	12.000 um
COLD OPTICS TRANSMISSION	0.857
COLD OPTICS EMISSIVITY	0.143
COLD OPTICS TEMPERATURE	75 K
UNSHIELDED STRUCTURE TEMPERATURE	75 K
UNSHIELDED STRUCTURE EMISSIVITY	1.000
UNSHIELDED SOLID ANGLE at DETECTOR	0.010 sr
CENTRAL OBSCURATION TEMPERATURE	75 K
CENTRAL OBSCURATION EMISSIVITY	1.000
COLD FILTER SPECTRAL TYPE (Wide : Narrow)	W
COLD FILTER CUT-ON WAVELENGTH	6.000 um
COLD FILTER CUT-OFF WAVELENGTH	9.000 um
COLD FILTER TRANSMISSION	0.910
COLD FILTER EMISSIVITY	0.050
COLD FILTER TEMPERATURE	20 K

OPTICS DATA:

COLLECTING OPTICS DIAMETER	20.0 cm
LINEAR OBSCURATION RATIO	0.000
POINT SOURCE COLLECTION EFFICIENCY (ref diff limit	1.000

DCWS 6-9 microns, 75 K, 20 msec frame time, .01 unshielded structure

INPUT DATA CONTINUED:

DETECTOR DATA:

DETECTOR MATERIAL (INSB, HGCDTE, SILICON)	Si:A
DETECTOR SIZE - AZIMUTH	75 um
DETECTOR SIZE - ELEVATION	75 um
DETECTOR THICKNESS	20 um
DETECTOR ACTIVE AREA RATIO (fill factor)	1.000
DETECTOR TEMPERATURE	10.0 K
DETECTOR CUTOFF WAVELENGTH	27.0 um
DETECTOR QUANTUM EFFICIENCY (default=TABLE)	0.5500
DETECTOR 1/f NOISE BREAK FREQ	0.000E+00 Hz
DETECTOR MODE (PV, PC, XX)(Default=PV)	PV
DETECTOR RoA PRODUCT (default=CALCULATED)	2.000E+06 Ohms.cm2
DETECTOR CAPACITANCE (default=TABLE)	5.0 pF
DETECTOR DARK CURRENT	0.000E+00 Amp

CHARGE INTEGRATING PREAMP INPUT DATA:

DETECTOR FULL WELL CAPACITY	1.000E+06 e-/pixel
ARRAY READ-OUT NOISE	50 e- rms

IRSENSOR VERSION 2.1 04/30/91

CURRENT DATE: 10/08/92
CURRENT TIME: 10:36

DCWS 9-12 microns, 75 K, 20 msec frame time, .01 unshielded structure

INPUT DATA

SENSOR DATA:

SENSOR TYPE (Stare:LinearScan:CircularScan)	S	
STARE TIME AVAILABLE	2.000E-02	sec
FIELD OF VIEW - AZIMUTH	4.326	degrees
FIELD OF VIEW - ELEVATION	4.326	degrees
IFOV - AZIMUTH	2.950E-04	radians
IFOV - ELEVATION	2.950E-04	radians
RANGE TO TARGET	100.0	km

RADIOMETRIC DATA:

BACKGROUND TYPE (Inband : Spectral : Greybody)	S	
BACKGROUND SPECTRAL RADIANCE	9.900E-11	W/cm2.sr.u
TARGET TYPE (Point : Xtended : Star)	P	
TARGET TEMPERATURE	300.0	K
TARGET AREA-EMISSIVITY PRODUCT	7.070E-01	cm2
FOREGROUND TYPE (Inband : Spectral)	I	
FOREGROUND INBAND RADIANCE	0.000E+00	W/cm2.sr
FOREGROUND TRANSMISSION	1.000	
WARM OPTICS TRANSMISSION	0.729	
WARM OPTICS EMISSIVITY	0.271	
WARM OPTICS TEMPERATURE	75	K
COLD OPTICS SPECTRAL TYPE (Wide : Narrow)	W	
COLD OPTICS CUT-ON WAVELENGTH	6.000	um
COLD OPTICS CUT-OFF WAVELENGTH	12.000	um
COLD OPTICS TRANSMISSION	0.857	
COLD OPTICS EMISSIVITY	0.143	
COLD OPTICS TEMPERATURE	75	K
UNSHIELDED STRUCTURE TEMPERATURE	75	K
UNSHIELDED STRUCTURE EMISSIVITY	1.000	
UNSHIELDED SOLID ANGLE at DETECTOR	0.010	sr
CENTRAL OBSCURATION TEMPERATURE	75	K
CENTRAL OBSCURATION EMISSIVITY	1.000	
COLD FILTER SPECTRAL TYPE (Wide : Narrow)	W	
COLD FILTER CUT-ON WAVELENGTH	9.000	um
COLD FILTER CUT-OFF WAVELENGTH	12.000	um
COLD FILTER TRANSMISSION	0.910	
COLD FILTER EMISSIVITY	0.050	
COLD FILTER TEMPERATURE	20	K

OPTICS DATA:

COLLECTING OPTICS DIAMETER	20.0	cm
LINEAR OBSCURATION RATIO	0.000	
POINT SOURCE COLLECTION EFFICIENCY (ref diff limit	1.000	

DCWS 9-12 microns, 75 K, 20 msec frame time, .01 unshielded structure

INPUT DATA CONTINUED:

DETECTOR DATA:

DETECTOR MATERIAL (INSB, HGCDTE, SILICON)	Si:A
DETECTOR SIZE - AZIMUTH	75 um
DETECTOR SIZE - ELEVATION	75 um
DETECTOR THICKNESS	20 um
DETECTOR ACTIVE AREA RATIO (fill factor)	1.000
DETECTOR TEMPERATURE	10.0 K
DETECTOR CUTOFF WAVELENGTH	27.0 um
DETECTOR QUANTUM EFFICIENCY (default=TABLE)	0.6500
DETECTOR 1/f NOISE BREAK FREQ	0.000E+00 Hz
DETECTOR MODE (PV, PC, XX)(Default=PV)	PV
DETECTOR RoA PRODUCT (default=CALCULATED)	2.000E+06 Ohms.cm2
DETECTOR CAPACITANCE (default=TABLE)	5.0 pF
DETECTOR DARK CURRENT	0.000E+00 Amp

CHARGE INTEGRATING PREAMP INPUT DATA:

DETECTOR FULL WELL CAPACITY	1.000E+06 e-/pixel
ARRAY READ-OUT NOISE	50 e- rms

IRSENSOR VERSION 2.1 - 04/30/91

CURRENT DATE: 09/21/92
CURRENT TIME: 11:22

FIRSSE 6-11 microns, 20 K, 6.5 msec frame time, .01 unshielded structur

INPUT DATA

SENSOR DATA:	
SENSOR TYPE (Stare:LinearScan:CircularScan)	S
STARE TIME AVAILABLE	6.500E-03 sec
FIELD OF VIEW - AZIMUTH	1.273 degrees
FIELD OF VIEW - ELEVATION	1.273 degrees
IFOV - AZIMUTH	8.680E-05 radians
IFOV - ELEVATION	8.680E-05 radians
RANGE TO TARGET	100.0 km
RADIOMETRIC DATA:	
BACKGROUND TYPE (Inband : Spectral : Greybody)	S
BACKGROUND SPECTRAL RADIANCE	7.200E-11 W/cm2.sr.u
TARGET TYPE (Point : Xtended : Star)	P
TARGET TEMPERATURE	300.0 K
TARGET AREA-EMISSIVITY PRODUCT	7.070E-01 cm2
FOREGROUND TYPE (Inband : Spectral)	I
FOREGROUND INBAND RADIANCE	0.000E+00 W/cm2.sr
FOREGROUND TRANSMISSION	1.000
WARM OPTICS TRANSMISSION	0.729
WARM OPTICS EMISSIVITY	0.271
WARM OPTICS TEMPERATURE	20 K
COLD OPTICS SPECTRAL TYPE (Wide : Narrow)	W
COLD OPTICS CUT-ON WAVELENGTH	6.000 um
COLD OPTICS CUT-OFF WAVELENGTH	16.000 um
COLD OPTICS TRANSMISSION	0.857
COLD OPTICS EMISSIVITY	0.143
COLD OPTICS TEMPERATURE	20 K
UNSHIELDED STRUCTURE TEMPERATURE	20 K
UNSHIELDED STRUCTURE EMISSIVITY	1.000
UNSHIELDED SOLID ANGLE at DETECTOR	0.010 sr
CENTRAL OBSCURATION TEMPERATURE	20 K
CENTRAL OBSCURATION EMISSIVITY	1.000
COLD FILTER SPECTRAL TYPE (Wide : Narrow)	W
COLD FILTER CUT-ON WAVELENGTH	6.000 um
COLD FILTER CUT-OFF WAVELENGTH	11.000 um
COLD FILTER TRANSMISSION	0.910
COLD FILTER EMISSIVITY	0.050
COLD FILTER TEMPERATURE	20 K
OPTICS DATA:	
COLLECTING OPTICS DIAMETER	36.0 cm
LINEAR OBSCURATION RATIO	0.480
POINT SOURCE COLLECTION EFFICIENCY (ref diff limit	1.000

FIRSSE 6-11 microns, 20 K, 6.5 msec frame time, .01 unshielded structure

INPUT DATA CONTINUED:

DETECTOR DATA:

DETECTOR MATERIAL (INSB, HGCDTE, SILICON)	Si:A
DETECTOR SIZE - AZIMUTH	75 um
DETECTOR SIZE - ELEVATION	75 um
DETECTOR THICKNESS	20 um
DETECTOR ACTIVE AREA RATIO (fill factor)	1.000
DETECTOR TEMPERATURE	10.0 K
DETECTOR CUTOFF WAVELENGTH	27.0 um
DETECTOR QUANTUM EFFICIENCY (default=TABLE)	0.5500
DETECTOR 1/f NOISE BREAK FREQ	0.000E+00 Hz
DETECTOR MODE (PV, PC, XX)(Default=PV)	PV
DETECTOR RoA PRODUCT (default=CALCULATED)	2.000E+06 Ohms.cm2
DETECTOR CAPACITANCE (default=TABLE)	5.0 pF
DETECTOR DARK CURRENT	0.000E+00 Amp

CHARGE INTEGRATING PREAMP INPUT DATA:

DETECTOR FULL WELL CAPACITY	1.000E+06 e-/pixel
ARRAY READ-OUT NOISE	50 e- rms

IRSENSOR VERSION 2.1 04/30/91

CURRENT DATE: 09/21/92
CURRENT TIME: 11:25

FIRSSE 11-16 microns, 20 K, 6.5 msec frame time, .01 unshielded structu

INPUT DATA

SENSOR DATA:

SENSOR TYPE (Stare:LinearScan:CircularScan)	S
STARE TIME AVAILABLE	6.500E-03 sec
FIELD OF VIEW - AZIMUTH	1.273 degrees
FIELD OF VIEW - ELEVATION	1.273 degrees
IFOV - AZIMUTH	8.680E-05 radians
IFOV - ELEVATION	8.680E-05 radians
RANGE TO TARGET	100.0 km

RADIOMETRIC DATA:

BACKGROUND TYPE (Inband : Spectral : Greybody)	S
BACKGROUND SPECTRAL RADIANCE	9.900E-11 W/cm2.sr.u
TARGET TYPE (Point : Xtended : Star)	P
TARGET TEMPERATURE	300.0 K
TARGET AREA-EMISSIVITY PRODUCT	7.070E-01 cm2
FOREGROUND TYPE (Inband : Spectral)	I
FOREGROUND INBAND RADIANCE	0.000E+00 W/cm2.sr
FOREGROUND TRANSMISSION	1.000
WARM OPTICS TRANSMISSION	0.729
WARM OPTICS EMISSIVITY	0.271
WARM OPTICS TEMPERATURE	20 K
COLD OPTICS SPECTRAL TYPE (Wide : Narrow)	W
COLD OPTICS CUT-ON WAVELENGTH	6.000 um
COLD OPTICS CUT-OFF WAVELENGTH	16.000 um
COLD OPTICS TRANSMISSION	0.857
COLD OPTICS EMISSIVITY	0.143
COLD OPTICS TEMPERATURE	20 K
UNSHIELDED STRUCTURE TEMPERATURE	20 K
UNSHIELDED STRUCTURE EMISSIVITY	1.000
UNSHIELDED SOLID ANGLE at DETECTOR	0.010 sr
CENTRAL OBSCURATION TEMPERATURE	20 K
CENTRAL OBSCURATION EMISSIVITY	1.000
COLD FILTER SPECTRAL TYPE (Wide : Narrow)	W
COLD FILTER CUT-ON WAVELENGTH	11.000 um
COLD FILTER CUT-OFF WAVELENGTH	16.000 um
COLD FILTER TRANSMISSION	0.910
COLD FILTER EMISSIVITY	0.050
COLD FILTER TEMPERATURE	20 K

OPTICS DATA:

COLLECTING OPTICS DIAMETER	36.0 cm
LINEAR OBSCURATION RATIO	0.480
POINT SOURCE COLLECTION EFFICIENCY (ref diff limit	1.000

FIRSSE 11-16 microns, 20 K, 6.5 msec frame time, .01 unshielded structur

INPUT DATA CONTINUED:

DETECTOR DATA:

DETECTOR MATERIAL (INSB, HGCDTE, SILICON)	Si:A
DETECTOR SIZE - AZIMUTH	75 um
DETECTOR SIZE - ELEVATION	75 um
DETECTOR THICKNESS	20 um
DETECTOR ACTIVE AREA RATIO (fill factor)	1.000
DETECTOR TEMPERATURE	10.0 K
DETECTOR CUTOFF WAVELENGTH	27.0 um
DETECTOR QUANTUM EFFICIENCY (default=TABLE)	0.6500
DETECTOR 1/f NOISE BREAK FREQ	0.000E+00 Hz
DETECTOR MODE (PV, PC, XX)(Default=PV)	PV
DETECTOR RoA PRODUCT (default=CALCULATED)	2.000E+06 Ohms.cm2
DETECTOR CAPACITANCE (default=TABLE)	5.0 pF
DETECTOR DARK CURRENT	0.000E+00 Amp

CHARGE INTEGRATING PREAMP INPUT DATA:

DETECTOR FULL WELL CAPACITY	1.000E+06 e-/pixel
ARRAY READ-OUT NOISE	50 e- rms

Appendix B

FIRSSE Cryogenic System Features Summary

FIRSSE Cryogenic System Design Summary
(ref. FIRSSE Final Report)

Feature	FIRSSE Design
Cryogen	Superfluid He (SfHe)
FPA Cooling Temperature	2K and 4K
FPA Cooling Design	Superfluid He via cooling ring conduction to dewar
Upper Baffle Cooling Temperature	< 15K
Upper Baffle Cooling Design	Superfluid He via cooling ring conduction to dewar
Background plate Cooling Temperature	19K (on inside of aperture cover)
Background plate Cooling Design	Superfluid He via cooling ring conduction to dewar when aperture cover is closed on sensor
Inner Rad.Shield Cooling Temperature	< 75K (inside structure of upper baffle, not "seen" by detector)
Inner Rad.Shield Cooling Design	He VCS cooling using dewar vent gas
Aperture Cover VCS Cooling Temperature	<100K (inside structure of cover, not "seen" by detector)
Aperture Cover VCS Cooling Design	conductively cooled by baffle VCS
Heat Loads: In-flight Aperture Load on He vapor cooling design	40W thermal pulse from payload structure as cap is removed and sensor is deployed 8W at first deployment angle (equal contribution from payload and earth) 11 W peak from earth at maximum deployment (earth contribution dominates)
Total Heat Leak to SfHe dewar (Parasitics)	0.56 W, aperture flux, conduction, radiation from outer structure
FPA load	< 1% of total heat leak to dewar or 6 mW
SfHe Hold time	maximum of 100 minutes
SfHe Fill/Hold conditions and calculation	1. Fill dewar - 17 liters at 2.7K to 3.0K just above lambda point 2. Pump vacuum on dewar then close vent line - reduces fluid to 15 liters SfHe 3. Launch conditions - 15 liters SfHe at 1.7K to 1.8K (7.9 torr) 4. Hold time from close of vent line to lambda point - maximum of 100 minutes 5. Hold time of 55 minutes planned for launch operations. 6. From launch to open of vent on-orbit is T+90 sec

The following questions and answers are based on discussions with Jim Lester on the FIRSSE design features many of which are shown earlier in this interim report in Figure 1. Some references are made to the FIRSSE final report..

o What is the "cooling ring on the dewar" - The ring is a cold interface ring-surface where telescope and FPA mount to the dewar. Has Al (five-9s) straps which are indium soldered to dewar cooling ring and VCS at lots of different locations. Telescope is also cooled with Al straps soldered to dewar cooling ring.

o Is the Inner radiation shield small baffle around quad and tert mirrors or is it the upper baffle? The inner radiation shield is the helium cooled VCS and upper baffle is conductively cooled. The temp sensor on "front end of the inner radiation shield" is called out as "aperture" on Figure 9 (FIRSEE final report) and is ~ 35K max. Is said to be "most sensitive to external thermal input". The temperature sensor is on front end/edge of inner radiation shield (VCS)

o Where is the aperture load absorbed? On the upper baffle or on the lower baffle? Aperture load is absorbed on the upper baffle which means it is conductively coupled to the SfHe dewar. This indicates the maximum load of 40W pulse at the aperture when the sensor starts deploying is absorbed by the SfHe. We would not have that load on the shuttle our loads were near 10W aperture loads.

o What cools the upper baffle? The baffle is conductively cooled with the Al straps.

o Is "background plate" which is on aperture cover sketch same thing as "sensor background plate" and background plate in Figure 10 (FIRSEE final report) which warms from 19K to over 80K when cover is open? Yes, the VCS behind it was conductively cooled with a contact joint (100 lbf) to the VCS but was only cooled when the cover was closed. When closed the inner background plate is conductively cooled by contact with the upper baffle and also must have been radiatively cooled by the cold telescope and upper baffle components.

o Is the purpose of the background plate just to reduce radiation parasitic load prior to start of observations? Yes, and to do sensor calibration.

o Is the background plate cooled via conduction down upper baffle to dewar? Yes.

Appendix 1

System Engineering Report No. DCWS-91.001.PS

Project: Debris Collision Warning Sensor
Subject: Visible End-to-End Performance Model
Prepared by: Paul W. Scott Date: January 10, 1991
Approved by: [signature] Date: 1/14/91

Abstract

This SER describes the end-to-end performance model on which the Debris Collision Warning Sensor Phase B Study is based. The model is implemented in a spreadsheet first developed under Lotus 1-2-3, and accepts as input many individual parameters of the target, background, geometry, optical system, and detector and produces predictions of numbers of debris particles seen by a sensor at 500 km altitude viewing in the horizontal direction. It is based on the current JSC debris model, documented in memorandum ES44-(193-90). The performance model has undergone many refinements during the Phase B Study, and can be easily modified to reflect other debris models or detection requirements. Currently, no particle is counted unless it is at sufficiently long range to produce a streak with both endpoints within a single field of view.

Analysis

Attachment A is an implementation of the spreadsheet for a frame transfer device. Originally, the spreadsheet simply calculated the SNR and some other performance parameters at a given range, particle size, etc. Now, the spreadsheet calculates the total number of particles counted per the DCWS requirements for a given sensor design. This section of this report walks through the spreadsheet and documents the elements within it. Each parameter has an item number, a terse description, a variable name, a value or formula, and units, where appropriate.

Items 1 through 6 are simply physical constants. Items 7 through 12 are inputs describing a particle. The range and particle radius can still be used to calculate a signal to noise ratio for a fixed set of conditions, but these parameters do not affect the particle count, since one must integrate over particle size and calculate the corresponding range in order to calculate total particle counts. The fixed values chosen for size and range are used to calculate the signal and noise contributions from which the values for other sizes and ranges are scaled. It is a check on this scaling process that the final results do not depend on the values chosen for the canonical particle. Item 13 is the visual magnitude of the canonical particle at the given size and range above. The equation for this magnitude is:

$$M_v(\text{particle}) = M_v(\text{Sun}) - 2.5\log_{10}[2\alpha r^2(\sin\phi+(\pi-\phi)\cos\phi)/(3\pi R^2)]$$

where α is the particle albedo, ϕ is the phase angle, r is the radius of the particle, and R is the range. From this value the irradiance from the particle (item 14) is calculated in photons/sec/m^2, assuming that the Sun emits 6.111×10^{21}

DISTRIBUTION: B. Burmester
B. Frank
D. Yates
F. Wargocki
P. Scott

photons/sec/m^2. Item 15 is the input number of equivalent 10th magnitude stars per square degree assumed spread out as a diffuse background. Item 16 is the calculated radiance of this background in photons/m^2/steradian/sec. The formula for this radiance is

$$N_b = (180/\pi)^2(6.111\times10^{21})[2.512^{M_v(Sun)-10}]$$

Items 17 through 22 are the input optical parameters. Items 19 through 22 determine the overall optical efficiency.

Items 23 through 39 are input parameters for the detector array. Item 27, the detector temperature, is not currently used, but could be used to scale the dark current. The number of "taps" in the case of the frame transfer devices refers to the number of independent frame transfer devices butted together in each direction to form the focal plane array. The numbers of pixels in items 24 and 25 refer to the entire focal plane array. Item 32, the parallel transfer time is the time required to move the electrons in the pixels one pixel in the parallel registers. The serial transfer time (item 33) is the time required to move a packet of charge one pixel in the serial register. These parameters determine the dead time, and limit the time available for readout through the preamp. This depends on whether the parallel registers run in the direction of the maximum binning or perpendicular to it. The particles are assumed in this model to move in the x or horizontal direction. The value in item 34 determines whether this direction is parallel to the parallel readout direction (1) or the serial readout direction (0). The dead time (item 35), expressed as percentage of the frame time, is just the amount of time required to shift all of the pixels out of the frame between integration times. It is the number of pixels in one parallel register of one device times the parallel read time times the frame rate, since the serial reads are accomplished during the next integration time. The read noise in item 36 is an input in electrons/square-root-Hz. The rms read noise scales as the square root of the inverse of the macropixel readout time over a limited range. The dark current (item 37) is an input parameter that is a function of detector temperature. Instead of being an input parameter, this number could be entered as a function of the detector temperature (item 27). Items 38 and 39, refer to the number of micropixels binned in the vertical and horizontal directions, respectively, to form a macropixel.

The only operational parameter included in the model is the number of equivalent continuous 7-hour observation periods assumed for taking data for the cross-plane case.

Items 41 through 52 are instrument parameters calculated from the above inputs. All the items are calculated in the obvious way except item 49. This parameter represents the inverse of the time allowed for the output preamp to read a single macropixel, and determines the read noise. The time allowed for this operation is determined by the integration period (for the next frame) and the number of macropixels in a single device, modified by the overhead required for parallel and serial transfers. The formula for this read "rate" is

$$FR*N_{mpt}/(1-2*DT-FR*N_{mpt}*BIN_s*T_s)$$

where FR is the frame rate, N_{mpt} is the number of macropixels per device (tap), DT is the dead time, BIN_s is the number of pixels binned into a macropixel in the serial direction, and T_s is the serial transfer time. The integration time in item 51 is simply the inverse of the frame time multiplied by the quantity 1 minus the dead time. The dwell time (item 52) is the IFOV for single micropixel (item 42) times the number of pixels binned in the horizontal direction (item 39) divided by the angular velocity of the particle based upon the nominal range (item 9). This dwell time is only valid for this range.

Items 53 through 74 are the focal plane performance results and some parameters required to calculate the table at the end of the spreadsheet, which calculates the maximum range for each particle size, the number of particles within that range and within the field of view, and the number of these particles that are outside the minimum range required for velocity measurement. Item 53 is the signal from the standard particle in photoelectrons, obtained by multiplying the photon irradiance from the particle by the area of the aperture times the macropixel dwell time times the optical efficiency times the detector quantum efficiency. The background photoelectrons collected are calculated in a similar way, except that the integration time is used instead of the dwell time, and the background radiance must be multiplied by the IFOV of a macropixel. The background noise is assumed to be the photoelectron shot noise associated with this level, or the square root of item 54. The read noise is just the read noise per root Hz (item 36) times the square root of the read rate calculated in item 49. The dark noise is the shot noise due to the dark current, and is therefore equal to the square root of the dark current per m^2 multiplied by the area of the detector, converted from amps to electrons per second and multiplied by the frame time. In item 58, the background, readout, and dark current parts of the noise are added in quadrature (root-sum-squared) to form the signal-independent part of the noise. This part does not scale with range or size of the particle. The signal-to-noise ratio in item 59 is the signal-to-noise ratio for the particle at the assumed range. One assumption has been made, which is that the integration of signal is dwell-time limited and not integration time limited. This is the case for the short range particles. Item 73 gives the maximum range for which this assumption is valid. If this assumption is not valid for the range selected in item 7, the particle count calculations from the tables will be correct, but this signal-to-noise ratio will be overestimated. The streak length in item 60 is the number of fundamental pixels traversed by the image of a particle going at the specified velocity in the horizontal direction during an integration time. This value may be more than the number of pixels in the array. The streak magnitude in item 61 is the particle magnitude reduced by 2.5 times the log of the number of macropixels in the streak, again not limited by the width of the array. The single frame streak signal to noise ratio (item 62) is the signal to noise ratio calculated above for a single macropixel multiplied by the square root of the number of macropixels in the streak, possibly limited by the width of the array. The multiple frame signal to noise ratio (item 63) is the single macropixel signal to noise ratio multiplied by the number of macropixels in the width of the array, and reduced by the square root of (1-DT) if the particles covers less than the width of the array in the integration time. <u>If the range is chosen to just meet the signal-to-noise requirements for detection</u>, then the "fishing net" calculated in item 64 is the virtual area in space subtended by the field of view cut to that maximum range. It is reduced by a factor of (1-DT) for particles which can cross the entire field of view in an integration time. This parameter is used to make a simple calculation of the debris count (item 69), given a uniform debris flux in a case where a simple power law describes the range vs. particle size. It is not used to get the debris counts given in the table, which allows for exceptions to these givens.

Items 65 and 66 are the peak and average data rates coming off the focal plane in macropixels per second. The reason they are different is that the process of reading out the array requires delays for parallel and serial transfers.

Items 67 and 68 are estimates of velocity and streak orientation accuracy based upon the canonical particle size and range. They do not apply to the collection of particles counted. The velocity accuracy is estimated simply by the horizontal binning figure (the number of pixels binned in the horizontal direction to form a macropixel) divided by the number of pixels in the streak, provided the streak is shorter than the frame. This assumes that the accuracy is limited by the resolution at which the endpoints of a single frame streak are measured. For very slow particles, the velocity would be estimated based on a number of frames as the particle crosses the field of view, and this number would be erroneous. A more correct model has been developed separately for this parameter. The model also assumes that the streak is precisely in the horizontal direction, and that both endpoints are within the field of view. The streak orientation accuracy is assumed to be taken on the basis of the composite streak as the particle traverses the entire field of view. It is simply the angle determined by the vertical bin size over the width of the field of view. Both the velocity accuracy and orientation accuracy estimates are somewhat crude and do not universally apply. They should therefore be used with caution. The 100% error shown in Attachment A is because the canonical particle is at a range that is too small for the velocity to be measured.

Items 70 - 74 are intermediate values used in the particle counting table below. The method used is to scale the calculations above to derive the range at which the signal-to-noise ratio equals one for each particle diameter. The scaling law depends upon whether the dwell time is longer or shorter than the integration time. In the table, the second column is an intermediate result. The three columns marked Int(d83), Int(d^4), and Int(1) are integrals of the debris model between each diameter and the next highest, and the column used depends upon whether the range is less than the range for which the integration time is equal to the dwell time, longer than this range, or longer than the maximum range for which there are particles. A lookup table is used to calculate the correct factor to correct for the fact that the debris density varies with altitude above the earth, and thus with range. For each particle count number, a certain percentage is greater than the minimum range for which velocity can be measured, taken to be the range at which the given velocity particle tranverses more than half the field of view in an integration time. This percentage is given in the next to last column of the count table which is on the fourth page of printout in Attachment A. The last column is simply the number of counts in the earlier column multiplied by the fraction whose velocity can be measured. At the bottom of the particle counting table (shown on the third page of the printout in Attachment A) is a summary of the particle counts in specific size ranges, both uncorrected and corrected for the fraction whose velocity cannot be measured. The number of particles which are greater than 10 cm is calculated on the assumption (which can be verified by reference to the table) that the maximum range for a 10 cm particle is beyond the end of the debris environment, 4784 km.

A couple of comments should be made about the method of calculating the counts. Up to the range at which the dwell time is as long as the integration time, the scaling equation is correct and reflects the fact that the range at which a particle can be seen grows as the particle diameter squared, based on a single frame, single pixel signal to noise ratio of 1. Beyond that range, the assumption is that multiple frames are co-added, for the number of frames that the particle stays on one pixel, to obtain the signal to noise ratio of 1. The model for this case is slightly incorrect when there is significant signal-dependent noise. This is due to the fact that instead of assuming that the signal to noise ratio is multiplied by the square root of the number of frames co-added, it was assumed that the number of signal photons was multiplied by this factor, including the photons that cause the shot noise, but not including the other noise sources. This has the effect of making the analysis much simpler, and is conservative since it has the effect of enhancing the signal photon shot noise. There are three possible solutions to this situation. Correcting the error involves the solution of a cubic equation instead of a quadratic, and is somewhat cumbersome for implementation in the spreadsheet. Making the assumption that we do not co-add frames to get the required signal to noise ratio simplifies the analysis but penalizes the count somewhat. At this time, this penalty is not sufficient to eat up all of our margin, but it is significant. The third is to accept the spreadsheet as it is, which is a much smaller penalty in conservatism, but is technically incorrect. We have chosen the latter approach, as a slightly conservative approximation to take into account the effect of frame co-adding.

After the range at which the particle can be seen is calculated, the count is calculated by the following equation:

$$N = 7.99x10^{-4} * Ndays * FOV_v/2 * (1-DT) * \int_{D_1}^{D_2} R^2(D) Flux(D) F(R(D)) dD$$

where $7.99x10^{-4}$ is the number of years in a 7-hour observing day, Ndays is the number of 7-hour observing days, FOV_v is the vertical field of view, DT is the dead time, R(D) is the range as a function of particle diameter D, Flux(D) is the non-cumulative flux distribution in particles per square meter per year per cm of diameter. The integral is taken over the range from the diameter for that line in the spreadsheet (D_1) to the diameter for the next line (D_2). F(R(D)) is a correction factor, calculated in MathCAD and implemented by means of a lookup table, which accounts for the flux variation as a function of altitude (range). The lookup table is shown on the last page of Attachment A, where the first column is range in km and the second column is F. The way that the above integral is calculated in the spreadsheet is the following:

$$\int_{D_1}^{D_2} R^2(D) Flux(D) F(R(D)) dD = R^2(D_1)/D_1^{2P} \int_{D_1}^{D_2} D^{2P} Flux(D) dD * F(R(D_1))$$

assuming that $R(D)=R(D_1)*(D/D_1)^p$. This is the case for each of the cases analyzed. For example, for dwell times shorter than the integration time, p=2. For dwell times greater than the integration time with frame co-adding (and with our approximation) p=4/3. For ranges beyond the maximum debris range, p=0. If we do not co-add frames, p=1. $R(D_1)$ is calculated in column three of the counting table. The integrated values for $D^{2p}*Flux(D)$ for each size range are included in columns 4, 5, and 6, and were calculated using MathCAD, an example of which is included in attachment B. Removing F(R(D)) from the integral and using its value at D_1 is a justified approximation, since F is a slowly varying function of R which varies between 1 and about 1.5. Since the function is monotonically increasing, the approximation is conservative.

The percentage of particles whose velocity can be measured is the square of the ratio between the range at which the particle traverses half of the FOV in the integration time and the maximum range for that particle size. Since this function is also monotonically increasing, using the value at D_1 is also conservative.

Model usage and constraints

The model described refers to frame transfer devices. A similar model exists which refers to full frame devices. Also a version of this model exists which assumes that frames are not co-added. In general, the model conforms to the particle detection and counting assumptions for the DCWS program. It is a simple matter to change this model to account for different program assumptions. If the debris model is changed, all that is required is to re-run the MathCAD model to derive different values for the appropriate columns in the counting table and another MathCAD model must be re-run to derive the values for the lookup table of correction factors for density vs. range. If co-adding is not assumed, the difference is that another column of integrated values of the debris model is required, for p=1, and the equation in the count column must be changed slightly. If a different assumption is made relative to the counting of fast particles, the two columns of the counting table can easily be modified. Most other assumptions are reflected in the numbered input values. The major approximations made in the model are the following:

1) The debris flux does not vary over the field of view.
2) Other sources of noise than those described above are negligible.
3) Detection range is determined by a signal to noise ratio of one in a macropixel.
4) The shot noise is artificially enhanced somewhat in the case of particles dwelling on a pixel for longer than the integration time.
5) The number of counts is reduced by the factor (1-DT) representing the percentage of the frame time over which the detector is integrating. This is a conservative approach.
6) Above all, the description of the debris particles is quite simplified, assuming identical spherical particles travelling with identical velocities.

As mentioned earlier, the estimates of velocity measurement accuracy and streak orientation accuracy are crudely determined and depend upon other gross assumptions.

The procedure for using the spreadsheet in its nominal configuration is simply to fill in the unprotected cells with the parameters of the background, target, instrument, etc., as approprate and to look for the counts at the bottom of the spreadsheet. The protected cells in the spreadsheet contain other useful information. A graph can be plotted of the range vs. particle size by pressing the F10 button, although you may want to alter the graph title.

Conclusion

The model described represents a reasonably flexible and accurate model of the end-to-end performance of a frame transfer CCD device according to the groundrules developed for the DCWS program. It should be modifiable to describe other groundrules for programs which detect and count a random flux of easily describable particles.

Attachment A - Printout Example for DCWS End-to-End Visible Performance Model

DCWS End-to-end System Model - Frame transfer mode - Visible only

Description	Variable	Value	Units
Physical constants			
1 Speed of light	c	3.00E+08	m/sec
2 Planck's constant	h	6.63E-34	joule-sec
3 Boltzmann's constant	k	1.38E-23	joule/mol-K
4 Magnitude of sun	ms	-26.74	mv
5 Deg to rad conversion	Dtr	0.017453	rad/deg
6 Charge on electron	q	1.6E-19	coulombs
Scene parameters			
7 Range	Rp	6452	m
8 Velocity	v	10000	m/sec
9 Angular velocity	w	1.549907	rad/sec
10 Particle radius	rt	0.0005	m
11 Particle albedo	a	0.08	
12 Phase angle	P	15	deg
Calculated scene variables			
13 Particle magnitude	mp	12.03	Mvis
14 Irrad. from particle	Hv	1.89E+06	ph/sec/m^2
Background parameters			
15 Background	Ns10	100	S10
16 Background radiance	Vbk	4.03E+12	ph/m^2/ster/sec
Optics parameters			
17 Clear aperture diam.	D	0.6	m
18 Focal ratio	Fno	2	
19 Loss per surface	Refv	0.95	
20 On-axis obsc. ratio	Obs	0.21	
21 No. of surfaces	Nm	2	
22 Beamsplitter eff.	BS	0.87	
Detector parameters			
23 Pixel size	Ps	2.70E-05	m
24 No. of pixels(horiz.)	Nxv	840	
25 No. of pixels (vert.)	Nyv	840	
26 Quantum efficiency	QEv	0.28	
27 Detector temp.	Temp	-60	deg C
28 CCD well capacity	FW	3.00E+05	e-
29 Frame rate	FR	30	Hz
30 Number of taps in x	NTx	2	
31 Number of taps in y	NTy	2	
32 Parallel x-fer time	PRT	8.00E-06	sec
33 Serial transfer time	SXT	2.00E-07	sec
34 (1_x-para.,0_y-para.)	FF	1	(flag)
35 Dead time	DT	10.08%	
36 Read noise	RN	0.008944	e-/root-Hz
37 Dark current	Dkv	5.00E-14	amps/cm^2
38 No. of vert. bins	BINV	2	
39 No. of horiz. bins	BINH	8	
Operational parameters			
40 No. of 7-hour days	Ndays	2	
Calculated instrument parameters			
41 Eff. focal length	Efl	1.2	m
42 Pixel FOV	IFOV	2.25E-05	rad
43 FOV (horiz.)	FOVxv	1.08	deg

44	FOV (vert.)__________	FOVyv	1.08	deg
45	Total no. of pixels__	Npv	705600	
46	Number of macropixels	Nmp	44100	
47	No. of pixels per tap	Nptap	176400	
48	No. of macropix/tap__	Nmpt	11025	
49	Macropixel read rate_	RR	4.97E+05	
50	Optics efficiency____	EOv	0.620288	
51	Integration time_____	Tv	0.029973	sec
52	Dwell time___________	Tdv	0.000116	sec

Calculated focal plane results

53	Signal electrons_____	Sv	10.78	e-
54	Backgrd. electrons___	Bv	48.08	e-
55	Backgrd. noise_______	Nb	6.93	e-
56	Readout noise________	Nr	6.30	e-
57	Dark noise___________	Nd	0.28	e-
58	Signal-ind. noise____	SIN	9.37	e-
59	Signal-to-noise______	SNRv	1.08573	
60	Streak length________	L	2064.71	pixels
61	Streak magnitude_____	ms	18.06	Mvis
62	Str. SNR (1 frame)___	SNRs	11.13	
63	Streak SNR (n-frame)_	SNRm	11.13	
64	Fishing net__________	Fnet	3.54E+05	m^2
65	Peak data rate_______	DRp	1.66E+06	macropixels/sec
66	Average data rate____	DRav	1.32E+06	macropixels/sec
67	Velocity accuracy____	VA	100.00%	error
68	Orientation accuracy_	OA	0.14	degrees
69	Particle count_______	Pc	243	*
70	A-constant___________	Ac	1.80E-08	
71	E-constant___________	E	69582.38	
72	F-constant___________	F	89790539	
73	Rge. for I.T.<Dw. T._	Rz	1665185	
74	Min. rge. for vel.___	Rvel	33495.59	

*This estimate is only good for 1mm to 1cm under certain conditions

---

Diameter (m)		Range	Int(d83)	Int(d^4)	Int(1)	Counts
0.001	0.10	7037	3.26E-05	2.51E-06	6.79E-03	16.87
0.002	0.40	28149	2.09E-05	3.25E-06	9.28E-04	21.86
0.003	0.91	63335	1.57E-05	3.85E-06	2.71E-04	25.90
0.004	1.62	112595	1.27E-05	4.38E-06	1.10E-04	29.48
0.005	2.53	175929	1.08E-05	4.87E-06	5.43E-05	32.76
0.006	3.64	253338	9.48E-06	5.33E-06	3.03E-05	36.04
0.007	4.96	344822	8.50E-06	5.78E-06	1.85E-05	39.36
0.008	6.47	450379	7.74E-06	6.23E-06	1.20E-05	42.80
0.009	8.19	570011	7.15E-06	6.68E-06	8.25E-06	46.40
0.01	10.11	703718	1.30E-05	1.47E-05	1.02E-05	105.13
0.012	14.56	1013354	1.16E-05	1.65E-05	5.85E-06	124.43
0.014	19.82	1379287	1.07E-05	1.83E-05	3.65E-06	145.95
0.016	25.89	1754876	9.87E-06	2.00E-05	2.42E-06	149.83
0.018	32.77	2053288	9.24E-06	2.17E-05	1.68E-06	145.67
0.02	40.45	2362979	8.70E-06	2.34E-05	1.21E-06	141.04
0.022	48.95	2683182	8.22E-06	2.50E-05	8.96E-07	136.09
0.024	58.25	3013248	7.80E-06	2.65E-05	6.80E-07	131.59
0.026	68.37	3352620	7.43E-06	2.79E-05	5.27E-07	126.59
0.028	79.29	3700814	7.11E-06	2.94E-05	4.17E-07	122.27
0.03	91.02	4057404	3.27E-05	1.73E-04	1.20E-06	564.59
0.04	161.82	4784000	3.38E-05	2.52E-04	6.20E-07	281.13

0.05	252.84	4784000	4.35E-05	4.26E-04	4.62E-07	209.70
0.06	364.08	4784000	6.08E-05	7.42E-04	4.12E-07	187.10
0.07	495.56	4784000	8.32E-05	1.23E-03	3.86E-07	175.03
0.08	647.26	4784000	1.09E-04	1.89E-03	3.60E-07	163.55
0.09	819.19	4784000	1.35E-04	2.72E-03	3.33E-07	151.02
0.1	1011.34	4784000		.1-1 cm		291.474
				1-3 cm		1328.589
				3-10 cm		1732.113

N>10 cm if R(10) > 4784 km	2346.188
Corrected for fast particles	
.1-1 cm	240.3025
1-3 cm	1327.947
3-10 cm	1732.017

Counts		
16.97	0.00%	0.00
21.86	0.00%	0.00
25.90	72.03%	18.65
29.48	91.15%	26.87
32.76	96.38%	31.57
36.04	98.25%	35.41
39.36	99.06%	38.99
42.80	99.45%	42.57
46.40	99.65%	46.24
105.13	99.77%	104.89
124.43	99.89%	124.29
145.95	99.94%	145.86
149.83	99.96%	149.78
145.67	99.97%	145.63
141.04	99.98%	141.02
136.09	99.98%	136.07
131.59	99.99%	131.58
126.59	99.99%	126.57
122.27	99.99%	122.26
564.59	99.99%	564.55
281.13	100.00%	281.11
209.70	100.00%	209.69
187.10	100.00%	187.09
175.03	100.00%	175.02
163.55	100.00%	163.54
151.02	100.00%	151.02

Rmax	Ffactor
0	1.0000
100	1.0014
200	1.0055
300	1.0123
400	1.0217
500	1.0336
600	1.0479
700	1.0642
800	1.0823
900	1.1020
1000	1.1228
1100	1.1445
1200	1.1665
1300	1.1886
1400	1.2104
1500	1.2315
1600	1.2517
1700	1.2708
1800	1.2886
1900	1.3052
2000	1.3204
2100	1.3343
2200	1.3469
2300	1.3583
2400	1.3686
2500	1.3779
2600	1.3863
2700	1.3939
2800	1.4007
2900	1.4069
3000	1.4125
3100	1.4176
3200	1.4222
3300	1.4264
3400	1.4303
3500	1.4338
3600	1.4370
3700	1.4400
3800	1.4428
3900	1.4453
4000	1.4477
4100	1.4499
4200	1.4519
4300	1.4538
4400	1.4555
4500	1.4572
4600	1.4587
4700	1.4602
4800	1.4615

Attachment B - MathCAD Model for Weighted Integrals of Debris Model

$k := 0.6$ 'k-factor'

$q := .02$

$p := .05$

$t := 1995$ (year)

$h := 500$ km (altitude)

$S := 97$

$Psi := 1.07$

$$g1 := (1 + q)^{t-1988}$$

$$g2 := 1 + p\,(t - 1988)$$

$$\Phi 1 := 10^{\frac{h}{200} - \frac{S}{140} - 1.5}$$

$$\Phi := \frac{\Phi 1}{\Phi 1 + 1}$$

$$\Phi \cdot Psi = 0.717$$

$$F1(D) := 1.22 \cdot 10^{-5} \cdot D^{-2.5}$$

$$F2(D) := 8.1 \cdot 10^{10} \cdot (D + 700)^{-6}$$

$$C(D) := \sqrt{10^{e^{-\left[\frac{\log(D) - .78}{.637}\right]^2}}}$$

$$F(D) := k \cdot \Phi \cdot Psi \cdot (F1(D) \cdot g1 + F2(D) \cdot g2) \cdot C(D)$$

Cumulative particle flux in particles per square meter per year of size greater than D cm.

$$f(D) := -\left[\frac{d}{dD} F(D)\right]$$ Non-cumulative distribution

$i := 1 \,..\, 9$

$a_i := i \cdot .1 \qquad b_i := a_i + .1$

$$Answer_i := \int_{a_i}^{b_i} D^4 \cdot f(D)\, dD$$ (Weighted integral as required for End-to-end performance model)

$Answer_i$

$2.51 \cdot 10^{-6}$
$3.251 \cdot 10^{-6}$
$3.851 \cdot 10^{-6}$
$4.378 \cdot 10^{-6}$
$4.865 \cdot 10^{-6}$
$5.33 \cdot 10^{-6}$
$5.782 \cdot 10^{-6}$
$6.23 \cdot 10^{-6}$
$6.676 \cdot 10^{-6}$

Appendix 2

System Engineering Report No. DCWS-91-003.PS
Project: DCWS
Subject: End-to-end system modelling for IR performance for DCWS
Prepared by: Paul W. Scott Date: January 29, 1991
Approved by: Date: 2/20/91

Abstract

This SER documents the methods used to model the DCWS system performance in the two infrared channels. The method involves performing an analysis to determine the signal and noise terms for a fixed particle at a fixed range with a dwell time that is equal to a fixed integration time and scaling, similarly to the visible model, to get the maximum range for each particle size for dwell times that depend on the particle range. The model allows for other parameters to be scaled between the "canonical" case and the scaled cases, but our practice has been to make the other parameters match as well as possible. This modelling procedure is made necessary by the existence of an excellent IR system model which has the limitation of dealing only with fixed targets, i.e. targets whose dwell times are equal to the integration time for a staring system. The model has been extremely useful for trading off system options and, in particular, in determining the required effective temperatures of optics and unshielded structure in the telescope.

Analysis

The analysis is based upon a Ball proprietary program for IR sensor system analysis called IRSENSOR. It is currently in version 2. A schematic of the parts of the phenomenology which are specified as inputs to the program is shown in figure 1, and a listing of the output and input for a typical case is included as Attachment A. Inputs for each part can be specified in a number of convenient ways. For example, the background can be specified as a total inband radiance, a constant spectral radiance over a specified band, or an equivalent greybody radiance over a specified band at a specified temperature and emissivity. The target can be a point source at infinity or a finite distance, or it can be an extended source with a finite projected area. If it is a point source at infinity (star), it can be specified with a spectral or total inband flux density. If it is a point source at a finite distance, it can be specified as a spectral or total inband radiant intensity or as a greybody with a specified temperature and area-emissivity product. An extended target can be specified by a projected area and either an inband or spectral radiance, or a temperature and emissivity. The foreground can be given an arbitrary transmission and an arbitrary inband or spectral radiance.

The optics are divided into two sections, referred to as "warm" optics and "cold" optics, each of which can be at an arbitrary temperature, have an arbitrary transmission and emissivity. The warm optics come first. The cold optics can also have a finite

ORIGINAL PAGE IS
OF POOR QUALITY

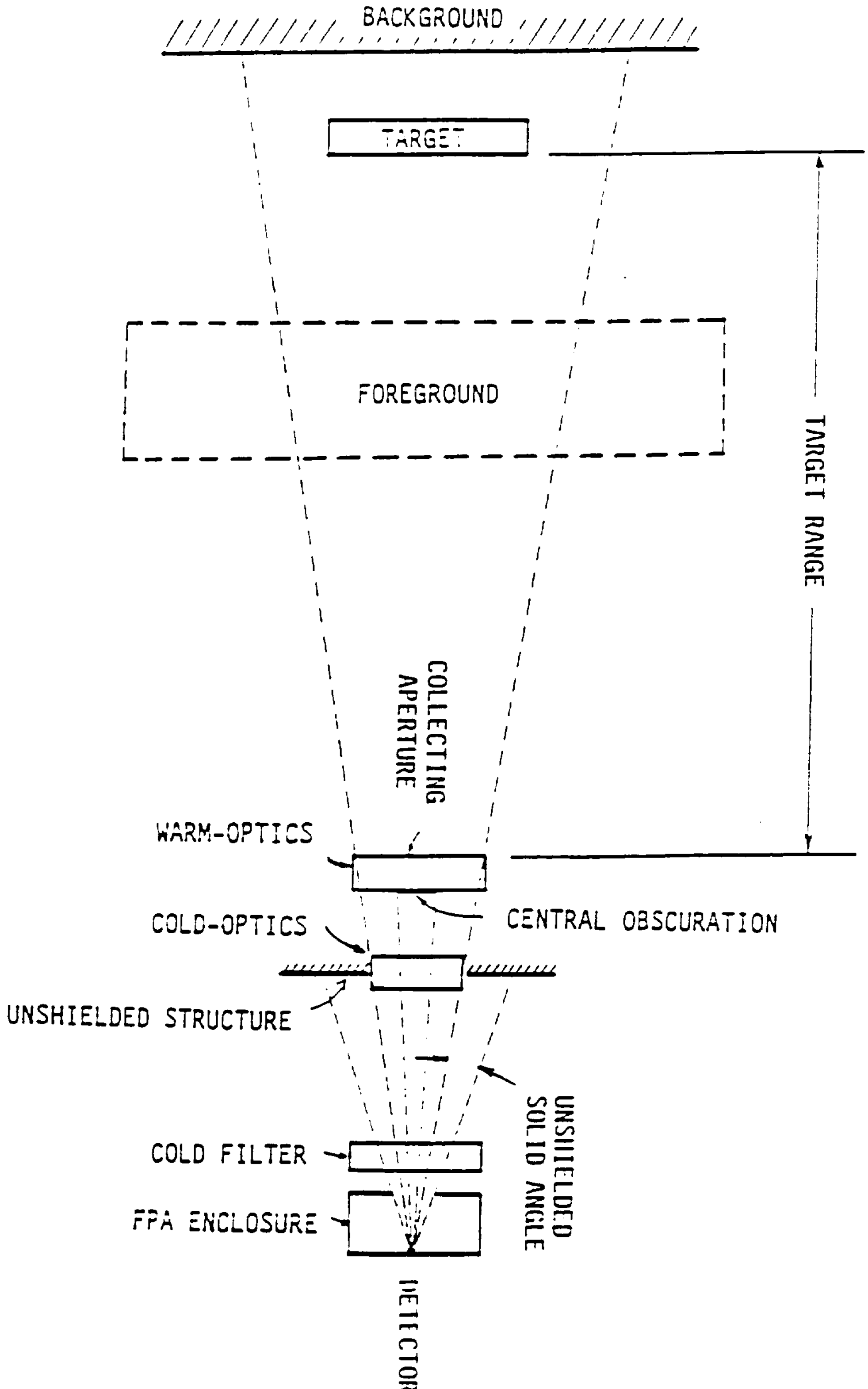

Figure 1

SCHEMATIC REPRESENTATION OF THE GENERAL IR SENSOR WHICH IS ANALYZED specified wavelength band. A cold filter in a cold shield is assumed as the last optical element in the system. The cold filter can have any temperature and emissivity itself and has a specifiable bandwidth and transmission. The detector is assumed to see photons from a specifiable central obscuration, the optics just described, a region of unshielded structure, and the cold shield outside the cold filter. Therefore we specify the unshielded structure temperature, emissivity, and solid angle outside the optical field of view (determined by the f/number) of the detector, but inside the cold shield. We must also specify the temperature and emissivity of the central obscuration. The cold optics spectral passband is applied only to the target, background, foreground, warm optics and central obscuration. The cold filter spectral passband is applied to these plus the cold optics and unshielded structure, but not to the cold filter itself.

The optics themselves are specified by collecting optics diameter, linear obscuration ratio, and point source collection efficiency. The collection efficiency is the ratio of the light falling on the detector, and the light that would fall on the detector if the system were diffraction limited. The program calculates the fraction of the light that would fall on the detector if the point source were centered on the detector and the system were diffraction-limited, including the effect of the central obscuration.

A wide variety of detectors can be modelled in IRSENSOR. If the material desired is HgCdTe, InSb, or intrinsic silicon, the program can be used to calculate typical performance parameters. If another material is used, or other measured parameters are required, these can be specified as well. The detector specification must include size (azimuth and elevation), active area ratio, thickness (only for gamma ray calculations), temperature, cutoff wavelength, quantum efficiency, R_0A, and capacitance, mode of operation (PV, PC, IB), photoconductive gain (1 for PV, 2 for PC, and arbitrary of IB), dark current, and 1/f noise break frequency. For detectors for which R_0A is not an appropriate quantity (photoconductive and impurity band conduction), one can compute an equivalent R_0A product.

The detector pre-amp can be either a trans-impedance amplifier, a charge integrating amplifier, or a source follower, as appropriate. Each has its own set of parameters. A charge integrating preamp is characterized by full well capacity and read-out noise, both measured in electrons. The simplified model of the TIA requires a preamp feedback resistance and capacitance (which can be calculated by the program), a maximum DC output voltage, an OpAmp open loop gain and unity gain bandwidth, an input FET white noise and 1/f noise break frequency, and a required preamp bandwidth. The source follower needs only an input white noise and 1/f noise break frequency.

In addition, both TIA's and source followers require a bandpass filter, whose characteristics must be specified. The characteristics can be calculated using a second companion program to IRSENSOR. The parameters required are upper and lower 3dB frequencies, high and low frequency roll-off rates, and lowest allowable filter transmission (for determining out-of-band rejection).

The program provides a variety of useful outputs. For our DCWS purposes, the single quantity of most interest is the peak signal to RMS noise ratio. However, for scaling purposes we need to use the signal photon level, the background photon level, the detector noise level, and the instrument thermal noise levels separately. These are also available in the output of IRSENSOR. For our purposes we have modelled the detector as an equivalent photovoltaic detector with a charge integrating preamp, having an R_0A product chosen to match measured D^* values.

Attachment B is a printout of the infrared system and target parameter scaling spreadsheet, IRSCALE. Its output and usage are similar to the visible end-to-end model (See SER No. DCWS-91-001), but it uses the output of the IRSENSOR program to establish the system performance parameters of a canonical system instead of deriving them from the instrument configuration. Items 1 through 8 are the parameters of the "canonical" system, which must match those of the system analyzed using IRSENSOR. Likewise, items 9 through 11 are parameters of the target. In the end, the range and diameter will be scaled to derive the number of detectable particles in each size bin. Item 12 is a signal to noise ratio from IRSENSOR which can be used to get a range for the scaled instrument and target based solely on this parameter under the assumption that the noise is signal-independent. While this is useful as a check, the final particle counts do not depend on this parameter, and it does not have to be filled in correctly.

Items 13 through 17 are the output values from IRSENSOR which determine the final result. Item 17, the signal shot noise, is used both to derive the signal and the noise due to it. Items 18 through 22 are parameters of the canonical system which are derived from items 1 through 8. These parameters also serve as a check.

Items 23 through 34 are the parameters of a new scaled system and target. This allows the results of IRSENSOR to be scaled to other system parameters. The exception to this is that the integration time cannot be scaled, and is set equal to the integration time for the canonical system. However, for the results presented on the DCWS program, we have modelled systems which are nearly identical to the final system with IRSENSOR, so that all these values match well with the canonical system, and reliance on the scaling laws is reduced. Items 35 through 39 are self-explanatory derived quantities of the new system.

Item 40 is the streak signal to noise ratio based on the desired signal to noise ratio on a pixel (item 26) and the number of pixels across the array. It is assumed to be a multi-frame quantity. The ratios in items 41 through 45 are the ratios of old and new system parameters. For example, item 45 is the ratio of the SNR calculated by IRSENSOR and the desired SNR. It is used to calculate item 48, the range based upon SNR. It is not used to calculate the count table. Since dwell time is proportional to range, item 46 expresses the additional dwell time associated with each unit of range. Item 47 is the range at which the dwell time is equal to the integration time.

Items 49 to 53 warrant some discussion, since these indicate how the signal and background noise terms are assumed to scale. The readout noise, Johnson noise, and instrument thermal noise are assumed not to scale at all. The background shot noise is assumed to scale only as the diameter of the telescope. The signal shot noise is assumed to scale as the diameter of the telescope and the diameter of the particle, and as the square root of the emissivity of the particle and the system efficiency.

The remainder of the numbered items are intermediate calculations used to calculate the count table, which is essentially identical to the table used for the visible model (See SER No. DCWS-91-001). There is one major difference however. All of the counts have been divided by 2, based upon the assumption that only half of the particles present have the analyzed temperature. In other words, we assume that the debris is divided evenly into two classes according to temperature, say 240K and 300K. The number calculated is the number in one class only which can be observed with the system. In fact, some members of the other class will be observed as well.

Model usage and constraints

Like the visible model, this model is geared to the DCWS requirements, but is also flexible for handling other requirements and constraints, including another debris model. As in the visible model the major approximations of the model are as follows:

1) The debris flux does not vary over the field of view.
2) Other sources of noise than those included in IRSENSOR are negligible.
3) Detection range is determined by a signal to noise ratio of one in a macropixel.
4) The shot noise is artificially enhanced somewhat in the case of particles dwelling on a macropixel for longer than the integration time. Since signal shot noise is seldom important for IR systems, this is generally a very small approximation.
5) The number of counts is reduced by the factor (1-DT) representing the fraction of time the detector is integrating. This is in general a somewhat conservative approach, but for the case of the baseline DCWS detectors it has no effect at all, since these detectors are read out directly, with no dead time between frames.
6) Above all, the description of the debris particles is quite simplified, assuming identical spherical particles travelling with identical velocities, and divided neatly into two temperatures.

The best procedure for using the model is to run IRSENSOR for a case as close as possible to the case at hand, with a selected range and particle size within the bounds of the problem. Then fill in the unprotected cells in the IRSCALE spreadsheet with the parameters of the old and new systems and the output signal and noise terms. The final counts appear at the bottom of the spreadsheet.

Conclusion

The modeling procedure described represents a reasonably flexible and accurate model of the end-to-end performance of an IR area array sensor, geared specifically to the DCWS requirements. It should be modifiable to apply to other sets of requirements for detecting and counting a random flux of easily describable particles.

Attachment A - Output example from IRSENSOR, showing input and output parameters.

[illegible]

CURRENT DATE: 1 12 [illegible]
CURRENT TIME: 18:40

DCMF 8-11 micron, 65 K, 10 msec frame time, .1 unshielded structure

INPUT DATA

SENSOR DATA:		
SENSOR TYPE (Stare:LinearScan:CircularScan)	S	
STARE TIME AVAILABLE	1.000E-02	sec
FIELD OF VIEW - AZIMUTH	0.500	degrees
FIELD OF VIEW - ELEVATION	1.110	degrees
IFOV - AZIMUTH	5.000E-05	radians
IFOV - ELEVATION	5.000E-05	radians
RANGE TO TARGET	1000.0	km
RADIOMETRIC DATA:		
BACKGROUND TYPE (Inband : Spectral : Greybody)	S	
BACKGROUND SPECTRAL RADIANCE	9.900E-11	W/cm2.sr.um
TARGET PRINT (Point : Xtended : Star)	P	
TARGET TEMPERATURE	300.0	K
TARGET AREA-EMISSIVITY PRODUCT	7.070E-01	cm2
FOREGROUND TYPE (Inband : Spectral)	I	
FOREGROUND INBAND RADIANCE	1.000E-00	W/cm2.sr
FOREGROUND TRANSMISSION	1.000	
WARM OPTICS TRANSMISSION	0.900	
WARM OPTICS EMISSIVITY	0.050	
WARM OPTICS TEMPERATURE	85	K
COLD OPTICS SPECTRAL TYPE (Wide : Narrow)	W	
COLD OPTICS CUT-ON WAVELENGTH	5.000	um
COLD OPTICS CUT-OFF WAVELENGTH	12.000	um
COLD OPTICS TRANSMISSION	0.950	
COLD OPTICS EMISSIVITY	0.050	
COLD OPTICS TEMPERATURE	85	K
UNSHIELDED STRUCTURE TEMPERATURE	75	K
UNSHIELDED STRUCTURE EMISSIVITY	1.000	
UNSHIELDED SOLID ANGLE at DETECTOR	0.100	sr
CENTRAL OBSCURATION TEMPERATURE	75	K
CENTRAL OBSCURATION EMISSIVITY	1.000	
COLD FILTER SPECTRAL TYPE (Wide : Narrow)	W	
COLD FILTER CUT-ON WAVELENGTH	9.000	um
COLD FILTER CUT-OFF WAVELENGTH	12.000	um
COLD FILTER TRANSMISSION	0.936	
COLD FILTER EMISSIVITY	0.050	
COLD FILTER TEMPERATURE	20	K
OPTICS DATA:		
COLLECTING OPTICS DIAMETER	80.0	cm
LINEAR OBSCURATION RATIO	0.500	
POINT SOURCE COLLECTION EFFICIENCY (ref diff limit	1.000	

ORIGINAL PAGE IS
OF POOR QUALITY

```
INPUT DATA CONTINUED:

DETECTOR DATA:
  DETECTOR MATERIAL (InSb, HgCdTe, SILICON)                      Si:A
  DETECTOR SIZE - AZIMUTH                                          100 um
  DETECTOR SIZE - ELEVATION                                        100 um
  DETECTOR THICKNESS                                                20 um
  DETECTOR ACTIVE AREA RATIO (fill factor)                       1.000
  DETECTOR TEMPERATURE                                            11.0 K
  DETECTOR CUTOFF WAVELENGTH                               [illegible] um
  DETECTOR QUANTUM EFFICIENCY (default=TABLE)              [illegible]
  DETECTOR R0A PRODUCT (default=CALCULATED)              1.000E-08 Ohms.cm2
  DETECTOR CAPACITANCE (default=TABLE)                             5.0 pF
  DETECTOR MODE (PV, PC, IB) (default=PV)                           PV
  DETECTOR PHOTOCONDUCTIVE GAIN (default=1)                       1.00
  DETECTOR EXCESS NOISE FACTOR (default=1)                        1.00
  DETECTOR DARK CURRENT                                  0.000E+00 Amp
  DETECTOR 1/f NOISE BREAK FREQ                          0.000E+00 Hz

CHARGE INTEGRATING PREAMP INPUT DATA:
  DETECTOR FULL WELL CAPACITY                            1.000E+06 e-/pixel
  ARRAY READ-OUT NOISE                                          50 e- rms
```

[illegible]

OUTPUT PARAMETERS

GEOMETRY DATA:	
NUMBER OF PIXELS - AZIMUTH	[illegible]
NUMBER OF PIXELS - ELEVATION	[illegible]
TOTAL NUMBER OF PIXELS PER FRAME OF DATA	[illegible]
PIXEL FOOTPRINT at TARGET RANGE - AZIMUTH	[illegible] km
PIXEL FOOTPRINT at TARGET RANGE - ELEVATION	[illegible] km
AREA OF PIXEL FOOTPRINT	8.888E-07 cm2
SOLID ANGLE SUBTENDED BY FOOTPRINT	8.888E-09 sr
DWELL TIME BASED ON GEOMETRY DATA	1.000E-02 sec
RANGE TO TARGET	1.000E-03 km
WAVELENGTH DATA:	
SYSTEM START WAVELENGTH	8.000 um
SYSTEM STOP WAVELENGTH	15.000 um
SYSTEM CENTER WAVELENGTH	11.500 um
SYSTEM SPECTRAL BANDWIDTH	6.000 um
WARNING : INPUT DETECTOR MATERIAL NOT INCLUDED	IN PROGRAM
DETECTOR DATA:	
DETECTOR AREA	1.000E-04 cm2
DETECTOR OPERATIONAL MODE	PV
DETECTOR PHOTOCONDUCTIVE GAIN	1.00
DETECTOR EXCESS NOISE FACTOR	1.00
DETECTOR DARK CURRENT	1.000E-09 Amp
DETECTOR DATA FROM STORED TABLES:	
DETECTOR MATERIAL SELECTED	Si:As
DETECTOR RoA PRODUCT	0.000E+00 Ohm.cm2
DETECTOR RESISTANCE	0.000E+00 Ohm
DETECTOR CAPACITANCE	0.0 pF
DETECTOR QUANTUM EFFICIENCY	0.0000
DETECTOR CUTOFF WAVELENGTH	20.0 um
DETECTOR DATA USED IN ANALYSIS:	
DETECTOR RoA PRODUCT	1.000E+06 Ohm.cm2
DETECTOR RESISTANCE	1.000E+10 Ohm
DETECTOR CAPACITANCE	5.0 pF
DETECTOR QUANTUM EFFICIENCY	0.8000
DETECTOR CUTOFF WAVELENGTH	20.0 um
OPTICS DATA:	
EFFECTIVE FOCAL LENGTH	120.48 cm
f/NUMBER AT DETECTOR	2.01
COLLECTING OPTICS AREA	2.827E+03 cm2
COLLECTING OPTICS A-OMEGA PRODUCT	1.948E-05 cm2.sr
AIRY DISC DIAMETER	4.270E-05 radians
AIRY DISC DIAMETER AT TARGET RANGE	4.270E-02 km
IFOV / AIRY DISC DIAMETER	1.944
DIFFRACTION LIMITED ENSQUARED ENERGY	0.851
ACTUAL ENSQUARED ENERGY	0.851
OPTICS SOLID ANGLE at DETECTOR	1.948E-01 sr
CENTRAL OBSCURATION SOLID ANGLE at DETECTOR	4.795E-02 sr
FPA ENCLOSURE SOLID ANGLE at DETECTOR	1.547E+00 sr
OPTICAL A-OMEGA PRODUCT at DETECTOR	1.948E-05 cm2.sr
UNSHIELDED STRUCTURE A-OMEGA PRODUCT	1.000E-05 cm2.sr
CENTRAL OBSCURATION A-OMEGA PRODUCT	4.795E-06 cm2.sr
FPA ENCLOSURE A-OMEGA PRODUCT	1.547E-04 cm2.sr

[illegible]

OUTPUT DATA CONTINUED:

RADIOMETRY DATA:

JOULES per PHOTON AT CENTER WAVELENGTH	[illegible] J/ph
TARGET PROJECTED AREA	[illegible] cm2
FRACTION OF FOOTPRINT OCCUPIED BY TARGET	[illegible]
FRACTION OF FOOTPRINT OCCUPIED BY BACKGROUND	[illegible]

EXTERNAL SOURCES:

BACKGROUND INBAND RADIANCE	2.970E-10 W/cm2.sr
BACKGROUND FLUX DENSITY WITHOUT TARGET	2.046E-18 W/cm2
BACKGROUND FLUX DENSITY WITH TARGET	2.046E-18 W/cm2
TARGET INBAND RADIANT INTENSITY	2.044E-08 W/sr
TARGET FLUX DENSITY	2.044E-19 W/cm2
FOREGROUND INBAND RADIANCE	0.000E+00 W/cm2.sr
FOREGROUND FLUX DENSITY	0.000E+00 W/cm2
TOTAL FLUX DENSITY WITHOUT TARGET	2.046E-18 W/cm2
TOTAL FLUX DENSITY WITH TARGET	2.250E-18 W/cm2
CHANGE IN FLUX DENSITY DUE TO TARGET	2.044E-19 W/cm2
INTRINSIC TARGET CONTRAST	9.990E-02

OPTICAL SYSTEM:	TRANSMISSION	THRUPUT W/ OBS
WARM OPTICS	0.900	0.675
COLD OPTICS	0.950	0.712
COLD FILTER	0.936	0.702
TOTAL	0.800	0.600

INTERNAL SOURCES:

WARM OPTICS INBAND RADIANCE AT FPA	1.754E-09 W/cm2.sr
COLD OPTICS INBAND RADIANCE AT FPA	1.847E-09 W/cm2.sr
UNSHIELDED STRUCTURE INBAND RADIANCE AT FPA	4.923E-09 W/cm2.sr
CENTRAL OBSCURATION INBAND RADIANCE AT FPA	4.677E-09 W/cm2.sr
COLD FILTER INBAND RADIANCE AT FPA	4.981E-20 W/cm2.sr
FPA ENCLOSURE INBAND RADIANCE AT FPA	1.158E-34 W/cm2.sr

DC CURRENT DATA:

DETECTOR Amp/Watt INCLUDING ACTIVE AREA RATIO — 6.769 Amp/Watt

DC CURRENTS AT DETECTOR OUTPUT:

DC BACKGROUND WITHOUT TARGET	2.349E-14 Amp
DC BACKGROUND WITH TARGET	2.349E-14 Amp
DC CURRENT DUE TO TARGET	1.997E-15 Amp
DC FOREGROUND	0.000E+00 Amp
DC CURRENT DUE TO WARM OPTICS	1.735E-13 Amp
DC CURRENT DUE TO COLD OPTICS	1.435E-13 Amp
DC DUE TO UNSHIELDED STRUCTURE	3.332E-13 Amp
DC CURRENT DUE TO CENTRAL OBSCURATION	1.518E-13 Amp
DC CURRENT DUE TO COLD FILTER	6.567E-24 Amp
DC CURRENT DUE TO FPA ENCLOSURE	2.232E-37 Amp
DC CURRENT DUE TO GAMMA FLUX	0.000E+00 Amp
DC CURRENT DUE TO DETECTOR DARK CURRENT	0.000E+00 Amp

TOTAL DC CURRENT WITHOUT TARGET	9.254E-13 Amp
TOTAL DC CURRENT WITH TARGET	9.274E-13 Amp
CHANGE IN DC CURRENT DUE TO TARGET	1.997E-15 Amp

TARGET CONTRAST AT DETECTOR OUTPUT	2.158E-03
PHOTON FLUX ONTO DETECTOR	7.243E+10 Ph/cm2.sec

ORIGINAL PAGE IS
OF POOR QUALITY

[illegible] UNSHIELDED STRUCTURE

OUTPUT DATA CONTINUED:

BANDPASS FILTER DATA:

FILTER UPPER 3dB FREQUENCY	[illegible]E-01 Hz
FILTER UPPER ROLL-OFF RATE	10.0 db/oct
FILTER LOWER 3dB FREQUENCY	[illegible] Hz
FILTER LOWER ROLL-OFF RATE	10.0 db/oct

CHARGE INTEGRATING PREAMP SNR DATA:

[16]	MAXIMUM DC CURRENT INTO CHARGE INTEGRATING WELL	8.274E-13 Amp
[16]	TIME TO SATURATE WELL	1.[illegible]E-01 seconds
	DWELL TIME TO AVOID SATURATION	1.000E-02 seconds
	NUMBER OF FRAMES WHICH COULD BE COADDED	1
	ARRAY READ-OUT RATE	1.4[illegible]E+06 pixels/sec
	ELECTRONS PER DWELL TIME PER AMPERE	6.2[illegible]E+16 e-/Amp

COLLECTED CHARGE per PIXEL:

	BACKGROUND CHARGE WITHOUT TARGET	1.468E+03 e-/pixel
	BACKGROUND CHARGE WITH TARGET	1.468E+03 e-/pixel
	COLLECTED CHARGE DUE TO TARGET	1.248E+02 e-/pixel
	COLLECTED CHARGE DUE TO FOREGROUND	0.000E+00 e-/pixel
	COLLECTED CHARGE DUE TO WARM OPTICS	1.084E+04 e-/pixel
	COLLECTED CHARGE DUE TO COLD OPTICS	1.522E+04 e-/pixel
	COLLECTED CHARGE DUE TO UNSHIELDED STRUCTURE	2.082E+04 e-/pixel
	COLLECTED CHARGE DUE TO CENTRAL OBSCURATION	9.487E-01 e-/pixel
	COLLECTED CHARGE DUE TO COLD FILTER	0.000E+00 e-/pixel
	COLLECTED CHARGE DUE TO FPA ENCLOSURE	0.000E+00 e-/pixel
	COLLECTED CHARGE DUE TO DETECTOR DARK CURRENT	0.000E+00 e-/pixel
	COLLECTED CHARGE DUE TO GAMMA FLUX	0.000E+00 e-/pixel
	TOTAL COLLECTED CHARGE WITHOUT TARGET	5.784E+04 e-/pixel
	TOTAL COLLECTED CHARGE WITH TARGET	5.796E+04 e-/pixel
[17]	CHANGE IN COLLECTED CHARGE DUE TO TARGET	1.246E+02 e-/pixel

DETECTOR/PREAMP/READOUT NOISE COMPONENTS:

DETECTOR JOHNSON NOISE	1.039E+02 e-rms
ARRAY READ-OUT NOISE	5.000E+01 e-rms
SHOT NOISE DUE TO DETECTOR DARK CURRENT	0.000E+00 e-rms
SHOT NOISE DUE TO GAMMA FLUX	0.000E+00 e-rms
TOTAL DETECTOR/PREAMP/READOUT NOISE	1.153E+02 e-rms

PHOTON SHOT NOISE COMPONENTS:

	SHOT NOISE DUE TO BACKGROUND WITHOUT TARGET	3.832E+01 e-rms
	SHOT NOISE DUE TO BACKGROUND WITH TARGET	3.832E+01 e-rms
	SHOT NOISE DUE TO TARGET	1.117E+01 e-rms
	SHOT NOISE DUE TO FOREGROUND	0.000E+00 e-rms
	SHOT NOISE DUE TO WARM OPTICS	1.041E+02 e-rms
	SHOT NOISE DUE TO COLD OPTICS	1.234E+02 e-rms
	SHOT NOISE DUE TO UNSHIELDED STRUCTURE	1.443E+02 e-rms
	SHOT NOISE DUE TO CENTRAL OBSCURATION	9.740E-01 e-rms
	SHOT NOISE DUE TO COLD FILTER	0.000E+00 e-rms
	SHOT NOISE DUE TO FPA ENCLOSURE	0.000E+00 e-rms
	TOTAL PHOTON SHOT NOISE WITHOUT TARGET	2.405E+02 e-rms
[illegible]	TOTAL PHOTON SHOT NOISE WITH TARGET	2.408E+02 e-rms

ORIGINAL PAGE IS OF POOR QUALITY

[illegible] - 11 microns, [illegible] K, 1.[illegible] frame time, [illegible] structure

CHARGE INTEGRATING PREAMP SNR SUMMARY:

```
WITHOUT CO-ADDED FRAMES:
[8]    TOTAL RMS NOISE WITH TARGET                          2.869E-02 e-rms
[9]    DC SIGNAL TO RMS NOISE RATIO             (SNR)       4.675E-01
[10]   NOISE EQUIV POWER at DETECTOR            (NEP)       6.304E-18 Watts
       DETECTOR DSTAR                           (D*)        2.686E-14 cm rootHz/W
[11]   SYSTEM DSTAR                             (D*)        1.100E-14 cm rootHz/W

       AT THE ENTRANCE APERTURE:
[12]     NOISE EQUIV FLUX DENSITY               (NEFD)      4.368E-19 W/cm2
         NOISE EQUIV SPECTRAL FLUX DENSITY      (NESFD)     1.456E-19 W/cm2.um
[13]     NOISE EQUIV RADIANCE                   (NEN)       5.394E-11 W/cm2.sr
         NOISE EQUIV SPECTRAL RADIANCE          (NESN)      1.798E-11 W/cm2.sr.um
[14]     NOISE EQUIVALENT TEMPERATURE DIFF.     (NEdT)      1.249E-06 K
         NOISE EQUIV SPECTRAL FLUX DENSITY (NESFDJY)        5.351E-02 Jy
         SPECTRAL NEFD EQUIVALENT STELLAR MAGNITUDE              7.110 mag

       AT THE TARGET RANGE:
         NOISE EQUIV FLUX DENSITY               (NEFD)      4.368E-19 W/cm2
         NOISE EQUIV SPECTRAL FLUX DENSITY      (NESFD)     1.456E-19 W/cm2.um
         NOISE EQUIV RADIANCE                   (NEN)       5.394E-11 W/cm2.sr
         NOISE EQUIV SPECTRAL RADIANCE          (NESN)      1.798E-11 W/cm2.sr.um
         NOISE EQUIVALENT TEMPERATURE DIFF.     (NEdT)      1.249E-06 K
[24]     NOISE EQUIV INBAND INTENSITY           (NEI)       4.368E-03 W/sr
         NOISE EQUIV SPECTRAL INTENSITY         (NESI)      1.456E-03 W/sr.um

WITH CO-ADDED FRAMES:
       SNR IMPROVEMENT BY CO-ADDING FRAMES                  1.000E+00
[18]   TOTAL RMS NOISE WITH TARGET                          2.869E-02 e-rms
[19]   DC SIGNAL TO RMS NOISE RATIO             (SNR)       4.675E-01
[20]   NOISE EQUIV POWER at DETECTOR            (NEP)       6.304E-18 Watts

       AT THE ENTRANCE APERTURE:
[21]     NOISE EQUIV FLUX DENSITY               (NEFD)      4.368E-19 W/cm2
         NOISE EQUIV SPECTRAL FLUX DENSITY      (NESFD)     1.456E-19 W/cm2.um
[22]     NOISE EQUIV RADIANCE                   (NEN)       5.394E-11 W/cm2.sr
         NOISE EQUIV SPECTRAL RADIANCE          (NESN)      1.798E-11 W/cm2.sr.um
[23]     NOISE EQUIVALENT TEMPERATURE DIFF.     (NEdT)      1.249E-06 K
         NOISE EQUIV SPECTRAL FLUX DENSITY (NESFDJY)        5.351E-02 Jy
         SPECTRAL NEFD EQUIVALENT STELLAR MAGNITUDE              7.110 mag

       AT THE TARGET RANGE:
         NOISE EQUIV FLUX DENSITY               (NEFD)      4.368E-19 W/cm2
         NOISE EQUIV SPECTRAL FLUX DENSITY      (NESFD)     1.456E-19 W/cm2.um
         NOISE EQUIV RADIANCE                   (NEN)       5.394E-11 W/cm2.sr
         NOISE EQUIV SPECTRAL RADIANCE          (NESN)      1.798E-11 W/cm2.sr.um
         NOISE EQUIVALENT TEMPERATURE DIFF.     (NEdT)      1.249E-06 K
[25]     NOISE EQUIV INBAND INTENSITY           (NEI)       4.368E-03 W/sr
         NOISE EQUIV SPECTRAL INTENSITY         (NESI)      1.456E-03 W/sr.um

              * (1 Jy = 1.0E-26 W/m2.Hz)
```

ORIGINAL PAGE IS
OF POOR QUALITY

Attachment B - Printout of IRSCALE spreadsheet for scaling of IRSENSOR results to predict particle counts

Infrared System and Target Parameter Scaling Spreadsheet

Canonical System Parameters (inputs)					
1	Clear aperture	Dc	0.6	m	
2	Pixel width	wc	1.00E-04	m	
3	Pixel height	hc	1.00E-04	m	
4	Pixel width IFOV	IFOVwc	8.30E-05	radians	
5	System efficiency	Effc	0.6	(Scales signal only)	
6	No. of pixels (width)	Nwc	105		
7	No. of pixels(height)	Nhc	231		
8	Integration time	Tic	0.01	sec	
Canonical Target Parameters (inputs)					
9	Range	Rc	1000000	m	
10	Diameter	Sc	0.01	m	
11	Emissivity	Epsc	0.9		
Canonical Figure of Merit Value					
12	Signal to noise ratio	SNRc	0.4875		
Canonical Noise Values					
13	Readout noise	RONc	50	e- rms	
14	Johnson noise	JNc	103.9	e- rms	
15	Background noise	BNc	38.31	e- rms	
16	Instr. thermal noise	TNc	237.4	e- rms	Does not scale!
17	Signal shot noise	SSNc	11.17	e- rms	
Derived Canonical System Parameters					
18	Eff. focal length	EFLc	1.20482	m	
19	Pixel height IFOV	IFOVhc	8.30E-05	rad	
20	FOV (width)	FOVwc	0.50	deg	
21	FOV (height)	FOVhc	1.10	deg	
22	Focal ratio (F/no.)	FNOc	2.01		
New System Parameters (inputs)					
23	Clear aperture	Dn	0.6	m	
24	Focal ratio (F/no.)	FNOn	2.00		
25	System efficiency	Effn	0.6		
26	Desired SNR	SNRn	1		
27	Dead time	DT	0		
28	No. of pixels (width)	Nwn	105		
29	No. of pixels(height)	Nhn	231		
30	Integration time	Tin	0.01		
New Target Parameters (inputs)					
31	Diameter	Sn	0.01	m	
32	Emissivity	Epsn	0.9		
33	No. of 7-Hour periods	N7	2	days	
34	Target velocity	Vn	10000	m/sec	
Derived New System Parameters					
35	Eff. focal length	EFLn	1.2000	m	
36	Pixel width IFOV	IFOVwn	8.33E-05	rad	
37	Pixel height IFOV	IFOVhn	8.33E-05	rad	
38	FOV (width)	FOVwn	0.50	deg	
39	FOV (height)	FOVhn	1.10	deg	
Derived performance parameters					
40	Streak SNR	SSNR	10.25		
41	Aperture ratio	Dr	1		
42	Emissivity ratio	Epsr	1		
43	System effic. ratio	Effr	1		
44	Particle diam. ratio	Sr	1		

ORIGINAL PAGE IS OF POOR QUALITY

45 SNR limit [illegible]	SNRr	[illegible]	
46 Dwell time/unit range	DTRr	8.36E-08	sec/m
47 Res. for Dw.T.=Int.T.	Rc	1000000	m
48 Range based on SNR	Rn	[illegible]	m

Parameters of stationary target at canonical range, new system

49 Readout noise	RONn	50	e- rms
50 Johnson noise	JNn	103.9	e- rms
51 Background noise	BNn	38.80	e- rms
52 Instr. thermal noise	TNn	237.4	e- rms
53 Signal shot noise	SSNn	11.17	e- rms

Intermediate calculations

54 Dw. time at nom. rnge	Tdn	0.008333	
55 Signal ind. noise	SINn	266.8379	e- rms
56 Dw.T.-ltd. sig. at Rc	SIG	103.9741	
57 E-constant	E	1.04E+08	
58 F-constant	F	1.14E-11	
59 Min range for vel.	Rmin	11428.57	

Size (m)		Range (m)	Int(d^3)	Int(d^4)	Int(1)	Counts
0.001	8.74E-05	8891.418	8.26E-05	2.51E-06	6.79E-03	2.82
0.002	1.50E-04	15565.66	2.09E-05	3.25E-06	9.28E-04	3.79
0.003	3.37E-04	35022.75	1.57E-05	3.85E-06	2.71E-04	4.48
0.004	5.99E-04	62262.88	1.27E-05	4.38E-06	1.10E-04	5.10
0.005	9.36E-04	97285.41	1.08E-05	4.87E-06	5.40E-05	5.67
0.006	1.35E-03	140091	9.46E-06	5.33E-06	3.03E-05	6.22
0.007	1.83E-03	190679.4	8.50E-06	5.78E-06	1.85E-05	6.74
0.008	2.40E-03	249050.6	7.74E-06	6.23E-06	1.20E-05	7.30
0.009	3.03E-03	315204.7	7.15E-06	6.68E-06	8.25E-06	7.87
0.01	3.74E-03	389141.6	1.30E-05	1.47E-05	1.02E-05	17.32
0.012	5.39E-03	560363.9	1.16E-05	1.65E-05	5.85E-06	19.84
0.014	7.34E-03	762717.6	1.07E-05	1.83E-05	3.65E-06	22.63
0.016	9.58E-03	996202.6	9.87E-06	2.00E-05	2.42E-06	25.69
0.018	1.21E-02	1240211	9.24E-06	2.17E-05	1.68E-06	28.59
0.02	1.50E-02	1427268	8.70E-06	2.34E-05	1.21E-06	25.97
0.022	1.81E-02	1620674	8.22E-06	2.50E-05	8.98E-07	25.39
0.024	2.16E-02	1820038	7.80E-06	2.65E-05	6.80E-07	24.80
0.026	2.53E-02	2025028	7.43E-06	2.79E-05	5.27E-07	24.21
0.028	2.93E-02	2235337	7.11E-06	2.94E-05	4.17E-07	23.63
0.03	3.37E-02	2450721	3.27E-05	1.73E-04	1.20E-06	110.23
0.04	5.99E-02	3596490	3.36E-05	2.52E-04	6.20E-07	119.46
0.05	9.36E-02	4784000	4.35E-05	4.26E-04	4.62E-07	118.76
0.06	1.35E-01	4784000	6.08E-05	7.42E-04	4.12E-07	105.96
0.07	1.83E-01	4784000	8.32E-05	1.23E-03	3.36E-07	99.13
0.08	2.40E-01	4784000	1.09E-04	1.89E-03	3.60E-07	92.62
0.09	3.03E-01	4784000	1.35E-04	2.72E-03	3.33E-07	85.53
0.1	3.74E-01	4784000		.1-1 cm		50.08
				1-3 cm		236.07
				3-10 cm		731.75
				Total		1017.91

N>10cm if R(10) > 4784 km	1134.81

Corrected for fast particles

.1-1 cm	44.30
1-3 cm	236.03
3-10 cm	731.75
Total	1012.08

Counts	[illegible]	Net
[illegible]	[illegible]	[illegible]
3.78	48.1[illegible]%	1.75
4.40	[illegible]	4.[illegible]
5.17	96.83%	4.96
5.27	98.80%	5.[illegible]
6.00	99.38%	6.17
6.74	99.64%	6.70
7.30	99.79%	7.02
7.57	99.87%	7.38
17.30	99.91%	17.30
19.54	99.96%	19.33
22.88	99.98%	22.88
25.69	99.99%	25.68
26.59	99.99%	26.59
25.97	99.99%	25.97
25.39	100.00%	25.39
24.80	100.00%	24.80
24.21	100.00%	24.21
23.63	100.00%	23.63
110.28	100.00%	110.28
113.46	100.00%	113.46
119.78	100.00%	119.73
105.96	100.00%	105.96
99.13	100.00%	99.13
92.62	100.00%	92.62
85.53	100.00%	85.53

Lookup table for spherical shell debris model

Tmax	Ffactor
0	1.0000
100	1.0014
200	1.0055
300	1.0123
400	1.0217
500	1.0336
600	1.0478
700	1.0642
800	1.0823
900	1.1020
1000	1.1228
1100	1.1445
1200	1.1665
1300	1.1886
1400	1.2104
1500	1.2315
1600	1.2517
1700	1.2708
1800	1.2886
1900	1.3052
2000	1.3204
2100	1.3343
2200	1.3469
2300	1.3583
2400	1.3686
2500	1.3779
2600	1.3863
2700	1.3939
2800	1.4007
2900	1.4069
3000	1.4125
3100	1.4176
3200	1.4222
3300	1.4264
3400	1.4303
3500	1.4338
3600	1.4370
3700	1.4400
3800	1.4428
3900	1.4453
4000	1.4477
4100	1.4499
4200	1.4519
4300	1.4538
4400	1.4555
4500	1.4572
4600	1.4587
4700	1.4602
4800	1.4615